Scientific report; WR 96-04

KNMI

Transformation of wind in the coastal zone

VN.N. Kudryavtsev
V.K. Makin

De Bilt, 1996

Scientific report = wetenschappelijk rapport; WR 96-04

De Bilt, 1996

Postbus 201
3730 AE De Bilt
Wilhelminalaan 10
Telefoon 030-220 69 11
telefax 030-221 04 07

UDC: 551.551.2
551.552
(210)

ISSN: 0169-1651

ISBN: 90-369-2108-2

© KNMI, De Bilt. Niets uit deze uitgave mag worden verveelvoudigd en/of openbaar gemaakt worden door middel van druk, fotocopie, microfilm, of op welke wijze dan ook, zonder voorafgaande schriftelijke toestemming van het KNMI.

Contents

Transformation of wind in the coastal zone

V.N. Kudryavtsev * and V.K. Makin
Royal Netherlands Meteorological Institute (KNMI)
De Bilt, The Netherlands

September 6, 1996

Abstract

A simple physical model of the wind transformation on an abrupt change in surface roughness and temperature across a coastal line is suggested. The model is based on a concept of the internal boundary layer (IBL) growth with fetch. It consistently describes both small scale (order of 1km) and mesoscale (order of 10-100 km) evolution of the IBL.

The planetary boundary layer problem (PBL) is solved using the similarity approach, which is applied for the IBL confined to the surface boundary layer, and the Ekman part of the PBL. A 3-layer eddy-viscosity model of the PBL is introduced for the description of the mesoscale evolution of the IBL.

The PBL model takes into account the baroclinicity effects due to the temperature gradient across a coastal line. Dynamical coupling with waves is a model option.

The model is verified on existing data and a reasonable agreement with observations is obtained. It is applied for the interpretation of a radar image of the sea surface and for the assessment of the wind transformation for typical atmospheric conditions at the Dutch coast. It is shown that the wind transformation has a significant impact on the wave growth in the coastal zone.

The model can be used as a module in multi-component coupled models describing dynamical processes in the ocean and the atmosphere and is viewed as a tool for engineering applications in the coastal zone.

1 Introduction

An off-shore wind, blowing from the land into the sea undergoes significant transformation due to an abrupt change in roughness and/or in temperature across a sea-land coastal line. The Internal Boundary Layer (IBL) develops with fetch on a typical spatial scale of about 100 km. On initial stages (typical fetch is 1km) the IBL growth is confined to the Surface

*Supported by the Netherlands Organisation for Scientific Research (NWO). On leave from the Marine Hydrophysical Institute, Sevastopol, Crimea, Ukraine

Boundary Layer (SBL). On later stages the IBL penetrates the SBL and develops further in the Ekman part of the Planetary Boundary Layer (PBL). Strong horizontal pressure gradients in a thermal internal boundary layer can cause strong jet-like surface winds on scales of few tens of kilometres. The air-sea interaction in the coastal zone (scale of 100 km) is determined to a great extent by peculiarities of the wind transformation. Therefore it is necessary to consider the evolution of the IBL in the study of coastal sea and atmosphere dynamics.

A proper description of the wind field in the coastal zone is important for many applications of ocean and atmosphere modelling. It is a known quality of the storm surge WAQUA model to underpredict negative surge in off-shore wind conditions, which can be caused by an inadequate description of the coastal winds. Modelling of wind wave growth near the coast requires the knowledge of coastal wind fields. Inadequate interpolation of winds to the nearest land-sea grid points in the WAM model can cause errors in the description of wave evolution and propagation. Calculations of the exchange coefficients of momentum, heat, water vapour and gases in the coastal zone require accurate estimates of coastal winds. The interpretation of field measurements of momentum, heat and moisture fluxes at near shore sites should take into account the influence of the developing IBL on the boundary layer structure.

Thus the description of the wind transformation in the coastal zone is necessary for understanding and modelling the initial growth of wind waves, the set up of a surge, the development of near shore currents, and the air-sea exchange of momentum, heat, water vapour and gases.

The description of the wind transformation requires a solution of the planetary atmospheric boundary layer (PBL) problem. The PBL is formed by a combined effect of the Coriolis force and the turbulent stress. The latter is a result of the dynamical and thermal interaction of the air flow with the underlying surface.

The first fruitful results related to the PBL theory were obtained within the framework of similarity theory by Kazanski and Monin (1960). The modern development of similarity theory of Kazanski-Monin was done by Zilitinkevich (1989).

In the present time major efforts to study the PBL have been made by numerical modelling based on the solution of the Reynolds equations. Reynolds stresses are parametrized by various closure hypotheses such as two-equation eddy-viscosity schemes, and second generation turbulent-stress models (Venkatram, 1977; Garratt ,1987; Garratt et al., 1995). Large-eddy simulation of the PBL is rapidly evolving (Deardorff, 1972; Mason, 1994; Garratt et al., 1995). However these models are very costly and their use is limited to specific scientific problems.

Simpler models of the PBL which are based on the ideas of similarity theory and some empirical knowledge (Brown, 1982; Garratt, 1987; van Wijk et al., 1990; Zilitinkevich, 1989a,b) are more attractive to engineering applications, and could be used as a simplified atmosphere module in coupled atmosphere- ocean models, coupled wind-waves and surge models, and in remote sensing algorithms.

The main goal of the present study is to develop a simple physical model of the PBL for the description of surface winds in the coastal zone. The model is designed as a module

for use in multi-component coupled models, describing various dynamical processes in the coastal seas and the atmosphere. The model is viewed as a tool for engineering applications in the coastal zone.

Despite the relative simplicity of the model it accounts for the main physical processes which determine the evolution of the PBL in the coastal zone: stratification effects, growth of the internal boundary layer or IBL on an abrupt change in roughness and/or temperature across the land-sea boundary and thermal sea fronts, baroclinicity effects (horizontal air temperature gradient). The model describes uniformly both the small scale (few kilometres from a shore) and the mesoscale (few tens to few hundreds kilometres) evolution of the IBL. The extension of the model makes it possible to describe the IBL evolution in complex domains: the transformation of wind across land-sea-land and sea-land-sea, as well as the transformation of an on-shore wind. The dynamical coupling with wind waves is one of the model's options.

The model is a semi-empirical one and is based on similarity theory of the surface boundary layer and an analytical description of the Ekman layer. The model generalizes the two-layer model of Brown (1982). The generalization (Kudryavtsev, 1995) is mainly related to the additional assumptions concerning the vertical distribution of the eddy-viscosity coefficient in the PBL in presence of the IBL. The similarity approach is used to solve the Ekman part of the PBL. The drag and heat geostrophic transfer laws are derived. They form a system of algebraic equations which is solved for the surface stress and its direction, heat flux and the height of the IBL. Profiles of the wind velocity and temperature are then calculated along fetch. The external parameters, which determine the solution, are of the free atmosphere (geostrophic wind and its direction, temperature), and temperature and roughness of the sea and of the land surface. These parameters are available from a regional atmospheric model and/or observations. Detailed description of the model is given in section 2.

In section 3 the model is verified on existing data of the geostrophic transfer coefficients, heights of the PBL and the IBL, the surface stress (wind) angle, profiles of the wind speed and temperature. A reasonable agreement with observations is found.

In section 4 the model is applied for the interpretation of a radar image of the sea surface and for the assessment of the wind and wave transformation for typical atmospheric conditions at the Dutch coast.

2 Model of the PBL transformation

2.1 Approach

The transformation of the atmospheric planetary boundary layer, forced by a step change in the surface roughness, temperature or humidity, is described using the internal boundary layer approach. The IBL is associated with the horizontal advection of the air across a discontinuity in some property of the surface. It is defined as a lower part of the PBL where the structure of turbulence is modified due to the interaction with the surface.

In the coastal zone an abrupt change in the surface roughness (the sea surface is much smoother compared to the land surface), and an abrupt change in temperature (the sea

surface can be much warmer in autumn and much colder in spring than the land surface), both determine the evolution of the IBL, and thus the coastal winds. The sea-land coastal line is defined here as a discontinuity line in the surface roughness and temperature.

Two main regimes are distinguished in the growth of the IBL. The small scale evolution of the IBL takes place on small fetches (few kilometres from a coast). The growth of the IBL is confined to the surface boundary layer. The mesoscale evolution takes place on scales of few kilometres to few hundreds kilometres, depending on the atmospheric stratification. The IBL penetrates the SBL and evolves in the Ekman part of the PBL. A comprehensive review on the IBL problem is given, e.g. in Garratt (1990).

This study is based on the 3-layer PBL model of Kudryavtsev (1995) which generalize the 2-layer PBL model of Brown (1982). We give a brief description of Brown's model in the next section (2.1.1), and its generalization in section 2.1.2.

We shall then develop the original model of Kudryavtsev (1995) in several ways. The main development concerns the description of the IBL growth on small fetches, i.e. the small scale evolution of the IBL, when the IBL growth confines to the SBL. The extensive description is given in section 2.2.

In section 2.3 the mesoscale evolution of the IBL is described. Compared to the model of Kudryavtsev (1995), the PBL equations for temperature and wind velocity are treated with advection terms. The approximate solution of these equations, which describe the IBL growth in the Ekman part of the PBL, is achieved here using the similarity approach.

The generalized equation for the IBL growth which uniformly describes the IBL evolution on both small scales and mesoscales, as well as wind and temperature profiles, and heat and wind velocity resistance laws are given in section 2.3.4.

A guide to the model is given in section 2.4.

2.1.1 Background model

We follow the approach of Brown (1982) to describe the structure of the equilibrium 'background' PBL. In the model of Brown (1982) the vertical structure of the PBL consists of two layers: the lower surface boundary layer of height h and the upper Ekman boundary layer of height D.

The SBL is described in terms of Monin-Obukhov similarity theory. The eddy-viscosity coefficient K increases linearly with height within this layer. The eddy-viscosity coefficient in the Ekman part of the PBL ($z > h$) is assumed to be constant with height and equals its value at the upper boundary of the SBL $z = h$:

$$K = \frac{\kappa u_* h}{\Phi_u(h/L)}, \tag{1}$$

where $\kappa = 0.4$ is the von Karman constant, u_* is the friction velocity, L is the Monin-Obukhov length scale, Φ_u is a universal similarity function (the dimensionless gradient) of the wind profile.

The eddy-viscosity K defines the vertical scale of the PBL (the Ekman depth):

$$H = \left(\frac{2K}{f}\right)^{1/2} = \frac{\kappa u_*}{f}\frac{1}{A(\mu)}, \tag{2}$$

where $\mu = \kappa u_*/fL$ is the stratification parameter. $A(\mu)$ is a dimensionless function which satisfies the equation:

$$A(\mu) = \frac{\Phi[\varepsilon\mu/A(\mu)]}{2\varepsilon}, \tag{3}$$

where $\varepsilon \sim 0.1$ is the main fitting parameter of the Brown (1982) model. This parameter defines the SBL height via the PBL scale H:

$$h = \varepsilon H. \tag{4}$$

The height of the PBL is also defined via the Ekman depth H: $D = mH$, where constant m is close to 2.

Overlapping the SBL and the Ekman part profiles and gradients of the wind velocity at height $z = h$ the resistance laws of the PBL can be obtained.

2.1.2 Generalization of a 2-layer background model: 3-layer model

The generalization is mainly related to the additional assumptions concerning the vertical distribution of the eddy- viscosity coefficient K, and accounts for the development of the IBL with fetch. The 3-layer K model is introduced to describe the IBL evolution in the Ekman part of the PBL.

On small scales, the height of the IBL δ is lower than the height of a new SBL $h(x)$. In this case the K-model is

$$K = \begin{cases} K(z,x) = \kappa u_* z \Phi_u^{-1}(z/L) & \text{if } z_0 < z < \delta(x) < h(x) \\ K(z,x) = K_0(z) & \text{if } \delta(x) < z, \end{cases} \tag{5}$$

where h_0 is the height of the background SBL. Hereafter subscript 0 denotes parameters of the background PBL. The universal dimensionless profile function Φ_u will be defined later. On small scales the IBL depth is less than the SBL height. The relation for K in the IBL is thus implies that wind and temperature profiles in the IBL can be described by the similarity theory of Monin-Obuchov. The structure of the atmosphere above the IBL height has the properties of the background PBL.

On mesoscales the height of the IBL exceeds the height of the SBL. The K-model is therefore

$$K = \begin{cases} K(z,x) = \kappa u_* z \Phi_u^{-1}(z/L) & \text{if } z_0 < z < h(x) \\ K(x) = K(h,x) & \text{if } h(x) < z < \delta(x) \\ K(z,x) = K_0(z) \equiv K_0 & \text{if } \delta(x) < z. \end{cases} \tag{6}$$

The upper boundary of the lower layer is defined as the height of the SBL, which is fully adjusted to the new surface. The structure of this layer ($z_0 < z < h(x)$) is formed

by the local fluxes of momentum and heat. In the SBL the eddy- viscosity K follows from the similarity theory of Monin- Obuchov. K depends on a height z, and implicitly, via the friction velocity u_*, on x - the distance from a coastal line.

The second layer is bounded by the SBL height $h(x)$ from below and the height of the IBL $\delta(x)$ from above. The structure of this layer ($h(x) < z < \delta(x)$) is formed by the local fluxes of momentum and heat at the height of the SBL and by the advection. In this layer K is constant over the height and equals its value at the height of the SBL $h(x)$. $K(h, x)$ depends indirectly on x via the local momentum and heat fluxes dependence on x.

The third layer is bounded from above by the height of the equilibrium PBL ($\delta(x) < z < D_0$). The eddy-viscosity K is defined by its equilibrium value K_0. If the IBL penetrates the height of the equilibrium PBL D_0, it evolves further in a non turbulent medium.

The 3-layer K-model (5) - (6) is a key assumption of the PBL model and determines its results.

Profiles of the wind speed and temperature follow from a solution of the balance equations of momentum and heat.

2.2 Small scale evolution of the IBL

The small scale evolution of the IBL, i.e. on relatively small fetches, where the IBL growth is confined to the SBL, forms the classical problem (Garratt, 1990). Two main questions to be answered are: how do wind and temperature profiles adjust to a step change in surface roughness and temperature, and how does the IBL grow. The key issue of this problem is to obtain an equation of the IBL height growth.

We shall first analyze the growth of the neutral IBL (section 2.2.1), then the growth of the thermal IBL (section 2.2.2), and finely end up with a uniform description of the IBL growth on a step change in surface roughness and temperature (section 2.2.3). Temperature and wind velocity profiles in the IBL and resistance laws are given in section 2.2.4.

2.2.1 Neutral IBL: growth across an abrupt change in roughness

The coastal line is assumed to coincide with the y-axis, the x-axis is perpendicular to the coast line and coincides with the wind direction.

The governing equations are:

$$\frac{\partial u^2}{\partial x} + \frac{\partial uw}{\partial z} = \frac{\partial \tau}{\partial z}, \tag{7}$$

$$\frac{\partial u}{\partial x} + \frac{\partial w}{\partial z} = 0, \tag{8}$$

where (u, w) are the horizontal and the vertical velocities, τ is the turbulent stress normalized on the density of the air.

The Karman-Polhausen method of integral constraint on the momentum balance of the IBL (Schlichting, 1979) is used to solve the equations and obtain $\tau(x)$, $u(z, x)$ and $\delta(x)$. The

integral method is based on the integration of eq. (7) from the surface to δ and substituting for w from eq. (8). That results in

$$\frac{\partial}{\partial x}\int_0^\delta u(u_\delta - u)dz - \int_0^\delta u dz \frac{\partial u_\delta}{\partial x} = \tau_\delta - \tau_s, \tag{9}$$

where u_δ and τ_δ are velocity and stress at height $z = \delta$, $\tau_s = u_*^2$ is the surface stress. According to the similarity theory the vertical distribution of velocity is given by

$$\frac{u(z)}{u_*} = \frac{1}{\kappa}\ln(\frac{z}{z_0}) + f(\frac{z}{\delta}), \tag{10}$$

where $f(z/\delta)$ is a universal function. We shall follow Elliott (1958) and Landau and Lifshits (1959), and set $f = 0$. The height of the IBL growth is then obtained from

$$\frac{\partial \delta}{\partial x} = 2\kappa\frac{\bar{u}_*}{u_\delta}\left(1 + O(\frac{\bar{u}_*}{u_\delta})\right), \tag{11}$$

where $\bar{u}_* = (u_* + u_{*0})/2$ is the mean friction velocity. If variations of $\bar{u}_*$ are not large, we can substitute $\bar{u}_* \simeq u_*$ in eq. (11) and solve it for the height of the IBL

$$\delta \simeq \frac{2\kappa^2}{\ln(\delta/z_0)}X. \tag{12}$$

Equation (12) agrees well with observations on small fetches, e.g. for laboratory conditions (Bradley, 1968; Garratt, 1990).

Multiplying eq. (11) by δ we can rewrite it in a form

$$u_\delta \frac{\partial \delta^2}{\partial x} = 4K_\delta, \tag{13}$$

where

$$K_\delta = \kappa u_* \delta \tag{14}$$

is the eddy-viscosity coefficient at height δ.

2.2.2 Thermal IBL: growth across an abrupt change in surface temperature

The thermal IBL or TIBL is formed on a step change in surface temperature.

To calculate its growth we shall use the equation of heat conservation

$$\frac{\partial u\theta}{\partial x} + \frac{\partial w\theta}{\partial z} = -\frac{\partial q}{\partial z}, \tag{15}$$

where θ is the potential temperature and $q = \overline{\theta' w'}$ is the kinematic heat flux. We again use the Karman-Polhausen method of integral constraint on the heat balance equation (15):

$$\frac{\partial}{\partial x}\int_0^\delta u(\theta_\delta - \theta)dz - \int_0^\delta u dz \frac{\partial \theta_\delta}{\partial x} = q_\delta - q_s, \tag{16}$$

where θ_δ and q_δ is temperature and the heat flux at height δ- the upper TIBL boundary, and $q_s = -\theta_* u_*$ is the surface heat flux. Using logarithmic wind and temperature profiles

$$u(z)/u_* = \frac{1}{\kappa}\left[\ln(\frac{z}{z_0}) - \Psi_u(z/L)\right], \tag{17}$$

$$\frac{\theta(z) - \theta_s}{\theta_*} = \frac{1}{\kappa}\left[\ln(\frac{z}{z_0 t}) - \Psi_\theta(z/L)\right], \tag{18}$$

where θ_s is the surface temperature, we can rewrite (16)

$$\bar{u}\left(\overline{d\theta}\frac{\partial\delta}{\partial x} - \delta\frac{\partial\theta_\delta}{\partial x}\right) = q_\delta - q_s. \tag{19}$$

In equation (19) $\overline{d\theta}$ and $\bar{u}$ are the mean wind speed and the mean temperature difference in the TIBL

$$\overline{d\theta} = \frac{1}{\delta}\int_{z_0}^{\delta}(\theta_\delta - \theta)dz \simeq \frac{\theta_*}{\kappa}\left[1 - \frac{1}{\delta}\int_{z_0}^{\delta}\left(\Psi_\theta(\delta/L) - \Psi_\theta(z/L)\right)dz\right], \tag{20}$$

$$\bar{u} = \frac{1}{\delta}\int_{z_0}^{\delta} u dz \simeq u_\delta. \tag{21}$$

Equations (20) and (21) are valid with an accuracy of $O(\theta_*/\kappa(\theta_\delta - \theta_s))$ and $O(u_*/\kappa u_\delta)$, respectively.

Universal dimensionless gradient and profile functions. The dimensionless profile functions Ψ_i, $i = [u, \theta]$ are related to the dimensionless gradients Φ_i by

$$\Phi_i(z/L) = 1 - \Psi_i'(z/L)\frac{z}{L}. \tag{22}$$

The dimensional gradients are defined by

$$\frac{\partial U}{\partial z} = \frac{u_*}{\kappa z}\Phi_u(z/L), \tag{23}$$

$$\frac{\partial \Theta}{\partial z} = \frac{\theta_*}{\kappa z}\Phi_\theta(z/L) \tag{24}$$

and are related to the eddy-viscosity K_i by

$$K_i = \frac{u_*\kappa z}{\Phi_i(z/L)}. \tag{25}$$

The dimensionless gradients are determined empirically from the flux-profile relations (23), (24). Widely accepted functional relations are (Dyer, 1974; Yaglom, 1977):

$$\Phi_u(z/L) = \left(1 - C_1 \frac{z}{L}\right)^{-1/4}, \quad z/L < 0, \tag{26}$$

$$\Phi_u(z/L) = 1 + C_2 \frac{z}{L}, \quad z/L > 0. \tag{27}$$

We use $C_1 = 16$ and $C_2 = 5$. For temperature the gradient relations are

$$\Phi_\theta(z/L) = \left(1 - C_3 \frac{z}{L}\right)^{-1/2}, \quad z/L < 0, \tag{28}$$

$$\Phi_\theta(z/L) = 1 + C_4 \frac{z}{L}, \quad z/L > 0, \tag{29}$$

and it is normally assumed that $C_3 = C_1$ and $C_4 = C_2$.

The profile dimensionless functions are then

$$\Psi_u(z/L) = 2\ln\frac{1+X}{2} + \ln\frac{1+X^2}{2} - 2\tan^{-1}X + \frac{\pi}{2}, \quad z/L < 0, \tag{30}$$

$$\Psi_u(z/L) = -C_2\zeta, \quad z/L > 0, \tag{31}$$

$$\Psi_\theta(z/L) = 2\ln\frac{1+X^2}{2}, \quad z/L < 0, \tag{32}$$

$$\Psi_\theta(z/L) = -C_4\frac{z}{L}, \quad z/L > 0, \tag{33}$$

where $X = (1 - C_1 z/L)^{1/4}$.

Growth of the TIBL in the near-neutral atmosphere. In this case conditions $|q_\delta| \ll |q_s|$ and $\partial\theta_\delta/\partial x = (\partial\theta_{\delta 0}/\partial z)(\partial\delta/\partial x) \simeq 0$ are realised and eq. (19) reduces to

$$\frac{\partial\delta}{\partial x} \simeq \frac{\kappa u_*}{u_\delta}\left[1 - \Psi'_\theta \cdot (\delta/L)\right]^{-1}\left[1 + \frac{1}{2}\frac{\Psi'_\theta \cdot (\delta/L)}{1 - \Psi'_\theta \cdot (\delta/L)}\right]^{-1} \simeq \frac{\kappa u_*}{u_\delta}\Phi_\theta^{-1}, \tag{34}$$

where $'$ denotes the derivative with respect to z/L at the level $z = \delta$. To derive eq. (34) we approximate $\Psi_\theta(\delta/L) - \Psi_\theta(z/L) \simeq -\Psi' \cdot (z - \delta)/L$.

The eddy-viscosity at height δ is

$$K_\theta(\delta) = \kappa u_* \frac{\delta}{\Phi_\theta(\delta/L)}, \tag{35}$$

and eq. (34) becomes

$$\bar{u}\frac{\partial}{\partial x}\delta^2 \sim 2K_\theta(\delta). \tag{36}$$

This equation has the same form as of Jensen et al. (1984), derived for the stratified atmosphere. In Van Wijk et al. (1990) the equation (36) was used with the proportionality

coefficient equal to 4, in order to obtain a better agreement with data. They used the eddy-viscosity coefficient for momentum. Notice, that for stable stratification $K_\theta = K$ (because $\Phi_\theta = \Phi_u$), while for unstable stratification $K_\theta \neq K$. The proportionality coefficient can be regarded here as a tuning parameter to bring results in conformity with data. The equation (36) will be used latter also with the coefficient equal to 4.

Growth of the convective TIBL in the stably stratified atmosphere. It is well known (Tennekes, 1973; Venkatram, 1977; Garratt, 1991) that when the convective IBL develops in the weakly turbulent, stably stratified atmosphere, the inversion temperature jump is formed at its upper boundary. The temperature jump across the inversion can be parameterized in the following way:

$$\Delta\theta \equiv \theta_0(\delta) - \theta(\delta) = \epsilon\gamma_0\delta, \tag{37}$$

where ϵ is a constant and γ_0 is the lapse rate in the background (undisturbed) atmosphere. The heat flux from the background atmosphere to the IBL due to the entrainment of the warmer air into the IBL is

$$q_\delta = -\Delta\theta\bar{u}\frac{\partial\delta}{\partial x}. \tag{38}$$

In the well mixed convective IBL the vertical change in temperature is negligible so that $\overline{d\theta} \sim 0$. Using this fact and eq. (38) the heat balance equation (19) can be written in the form

$$\bar{u}\left(\gamma_0\delta\frac{\partial\delta}{\partial x} - \delta\frac{\partial}{\partial x}\Delta\theta - \Delta\theta\frac{\partial\delta}{\partial x}\right) = q_s. \tag{39}$$

With (37) equation (39) reduces to

$$\bar{u}\frac{\partial}{\partial x}\delta^2 = \frac{2}{1-2\epsilon}\frac{q_s}{\gamma_0}, \tag{40}$$

which describes the growth of the IBL. Equation (40) gives the entrainment heat flux (38) in the form

$$q_\delta = -\frac{\epsilon}{1-2\epsilon}q_s. \tag{41}$$

Equation (41) corresponds to one of the convective IBL model of Tennekes (1973). The constant ϵ varies in the range of $0.15 \div 0.25$ according to experimental data and results of numerical modelling .

At the beginning stage of the IBL growth $q \sim C_H\bar{u}(\theta_s - \theta_{s0})$ (where $(\theta_s - \theta_{s0})$ is an abrupt change of surface temperature) and equation (40) can be rewritten

$$\delta \sim \left[\frac{2C_H}{1-2\epsilon}\right]^{1/2}\left[\frac{\theta_s - \theta_{s0}}{\gamma_0}\right]^{1/2} X^{1/2}. \tag{42}$$

Equation (42) describes the square root dependence of the IBL height on fetch X and is in agreement with data (see Raynor et al., 1975; Garratt, 1991) and results of Venkatram (1977) model.

Equation (40) becomes invalid when $\gamma_0 \to 0$. In this case the growth of the IBL is determined by equation (36) with the proportionality coefficient equals 4. We can merge (36) and (40) and obtain a relation which is valid for both cases

$$\bar{u}\frac{\partial}{\partial x}\delta^2 = \frac{2}{1-2\epsilon}K_\theta(\delta)\left(1+\frac{\gamma_0 K_\theta(\delta)}{q_s}\right)^{-1}, \tag{43}$$

where $\epsilon = 0.25$ is taken.

2.2.3 Transformation of the IBL across an abrupt change in roughness and temperature

In the coastal zone the IBL develops both due to abrupt changes in roughness (the sea is always smoother than the land) and due to abrupt changes in temperature (the sea is often warmer or cooler than the land). The stratification of the background atmosphere can be arbitrary and influence the IBL growth over the sea. To simulate the wind transformation in real conditions it is desirable to have a uniform description of the IBL growth. We shall introduce the generalized 'interpolation' equation for the growth of the IBL height. The generalized equation has to describe uniformly all possible regimes of the IBL development, and has to have the right asymptotic solutions in the special cases. Results have to be in agreement with data. The following generalized equation is suggested

$$\bar{u}\frac{\partial}{\partial x}\delta^2 = 4\alpha K(\delta), \tag{44}$$

where the eddy-viscosity coefficient at the height of the IBL δ is defined as

$$K(\delta) = \frac{\kappa u_* \delta}{\Phi(\delta/L)}, \tag{45}$$

and the growth rate parameter α is

$$\alpha = \left[1+\max\left(\frac{\gamma_0 K}{q_s}, 0\right)\right]^{-1}. \tag{46}$$

We shall illustrate the partial solutions of (44):

- When the background atmosphere is neutral ($\gamma_0 = 0$), the growth parameter $\alpha = 1$, and the equation (44) describes the growth of the IBL across an abrupt change in roughness (eq. (13)) and temperature (eq. (36)).
- When convective IBL develops in stably stratified atmosphere the ratio $\gamma_0 K/q_s \gg 1$ and $\alpha \simeq q_s/\gamma_0 K$. (We define $\gamma_0 = -q_0/K_0(\delta) = \partial\theta_0/\partial z$). Equation (44) reduces now to eq. (40).

- When the stratification of the IBL is close to the stratification of the background atmosphere the growth parameter $\alpha = 1$, because γ_0 and q_s have the opposite sign. Equation (44) describes the growth of the stratified IBL across an abrupt change in roughness. It generalizes equation (36), describing the IBL growth in the neutral atmosphere, in a sense that the dependence of the eddy-viscosity coefficient on the stratification is accounted for.

2.2.4 Profiles and resistance laws

We assume that the IBL is in a local equilibrium and its structure is defined by the local fluxes of momentum and heat:

$$u(z) = \frac{u_*}{\kappa}\left[\ln(\frac{z}{z_0}) - \Psi_u(z/L)\right], \tag{47}$$

$$\theta(z) = \theta_s + \frac{\theta_*}{\kappa}\left[\ln(\frac{z}{z_{0t}}) - \Psi_\theta(z/L)\right]. \tag{48}$$

The diabatic profiles of the wind speed and temperature are well established over the sea and land. The description of the IBL is fulfilled when the resistance laws for momentum and temperature are derived. For that the upper boundary condition at height δ has to be defined. We assume that the wind speed is continuous across the upper boundary of the IBL

$$u(\delta) = u^0(\delta). \tag{49}$$

Numerical experiments of Venkatram (1977) have shown that for the convective IBL the wind speed jump could be formed but it is small.

On the contrary, the temperature jump is formed across the inversion at the upper boundary of the convective IBL at $z = \delta$, and has to be taken into account. In other cases this temperature jump can be neglected. To satisfy all possible cases the upper boundary condition for temperature reads

$$\theta(\delta) = \theta^0(\delta) - \epsilon\gamma_0\delta \tag{50}$$

$$\epsilon = \max[0, 0.25\mathrm{sign}(\frac{\gamma_0 K}{q_s})]. \tag{51}$$

From (47) - (48) the resistance laws are

$$u_* = C_D^{1/2} u_\delta \tag{52}$$

and

$$\theta_* = C_H^{1/2}(\theta_\delta - \theta_s), \tag{53}$$

where the exchange coefficient for momentum (the drag coefficient) and heat (the Stanton number) are

$$C_D^{1/2} = \frac{\kappa}{\left[\ln(\frac{\delta}{z_0}) - \Psi_u(\delta/L)\right]}, \tag{54}$$

$$C_H^{1/2} = \frac{\kappa}{\left[\ln(\frac{\delta}{z_0 t}) - \Psi_\theta(\delta/L)\right]}. \tag{55}$$

A closed set of equations (44), (47)- (55) describes the spatial (in the x direction which is perpendicular to a coastal line) evolution of the IBL growth and defines the spatial distribution of momentum and heat fluxes. Wind and temperature profiles are defined by the local value of the friction velocity $u_*(x)$ and the temperature scale $\theta_*(x)$.

The IBL develops inside the SBL if the condition

$$\delta(X) \leq h \equiv \varepsilon H \tag{56}$$

is satisfied. The characteristic fetch when the IBL develops inside the SBL can be estimated from (44) and (56):

$$X_a \sim \frac{\varepsilon^2 G}{f} = 10^{-2}\frac{G}{f}, \tag{57}$$

where the geostrophic wind speed G is taken as a characteristic scale for the wind velocity. For $G = 10\text{m/s}$ and $f = 10^{-4}\text{s}^{-1}$ it results in $X_a = 1\text{km}$. The scale X_a defines the distance where the SBL is fully adjusted to the new surface.

When $X > X_a$ the IBL develops in the Ekman part of the PBL.

2.3 Mesoscale evolution of the IBL

A regime, when the IBL penetrates the height of the SBL and develops in the Ekman part of the PBL, is called the mesoscale evolution of the IBL. The vertical structure of the eddy-viscosity coefficient K is described by the 3-layer K-model, equations (6).

The PBL equations are listed in section 2.3.1. Assuming self- similarity in profiles of temperature and wind velocity in the Ekman part of the IBL, we obtain an approximate solution of the PBL equations (section 2.3.2). Some asymptotic regimes of the IBL evolution are discussed in section 2.3.3. We finally obtain the generalized equation of the IBL growth in section 2.3.4.

2.3.1 Equations

The eddy-viscosity coefficient for momentum and heat is constant with height in the Ekman part of the IBL. Equations for the conservation of heat and momentum in this case can be written in the form

$$\bar{u}\frac{\partial \theta}{\partial x} = K_\theta \frac{\partial^2 \theta}{\partial z^2}, \tag{58}$$

$$\bar{u}\frac{\partial U}{\partial x} + ifU = -\frac{1}{\rho}\Delta P + K\frac{\partial^2 U}{\partial z^2}, \tag{59}$$

where $\bar{u}$ is the x-component of wind velocity averaged over the depth of the IBL, $U = u + iv$ is the complex wind velocity, $\Delta = \partial/\partial x + i\partial/\partial y$, ρ is the air density, P is the pressure. The hydrostatic equation and the equation of state are

$$\frac{\partial P}{\partial z} = -\rho g, \tag{60}$$

$$P = \rho R T, \tag{61}$$

where T is temperature in Kelvin scale.

The relation between the pressure gradient at height z and the pressure gradient at the upper boundary of the IBL $\delta(x)$ follows from (60) and (61):

$$\frac{1}{\rho}\Delta P(z) = \frac{T(z)}{T(\delta)}\frac{1}{\rho_\delta}\left[\Delta P(\delta) + \rho g \Delta\delta\right] - \frac{g}{\overline{T}}\int_z^\delta \frac{\partial\theta}{\partial x}dz, \tag{62}$$

where $\overline{T}$ is the mean temperature in a layer from z to δ. The geostrophic wind velocity is defined by

$$ifG = -\frac{T(z)}{T(\delta)}\left[\frac{1}{\rho}\Delta P(\delta) + g\Delta\delta\right]. \tag{63}$$

Hereafter $G = G_x + iG_y$ is the complex geostrophic wind speed which is spatially homogeneous. The vertical heat flux q is defined as

$$q = -K_\theta \frac{\partial\theta}{\partial z}, \tag{64}$$

and with (58) equation (59) can be rewritten in the form

$$\bar{u}\frac{\partial U}{\partial x} + if(U - G) = K\frac{\partial^2 U}{\partial z^2} + \frac{g}{\overline{T}\,\bar{u}}\left[q(z) - q(\delta)\right]. \tag{65}$$

The second term on the r.h.s. of equation (65) describes the baroclinicity effect on the wind field. As it follows from (65) the baroclinicity term increases towards the surface and reaches its maximum at the height of the SBL ($z = h$). The baroclinicity term causes a thermal wind. In this case the thermal wind is induced by the pressure component resulting from the IBL evolution on an abrupt change in temperature across the coastal line. The scale of the thermal wind U_T is

$$U_T = \frac{g}{\overline{T}}\frac{q_s}{f\bar{u}}. \tag{66}$$

In eq. (66) q_s is the surface heat flux. (As in the SBL the heat flux is constant with height its surface value equals the heat flux at the lower boundary of the Ekman part of the IBL $q(h)$.) The baroclinicity effect is most pronounced for the wind blowing along the coastal line $\phi \to \pi/2$, as $\bar{u} = |\vec{U}|\cos\phi$. For the temperature difference of 10^o and the heat exchange coefficient $C_H = 10^{-3}$ the thermal wind speed $U_T = 3$ m/s for a wind blowing perpendicular to the coastal line and increases to 6 m/s if the wind direction changes to $\phi_s = 60^o$.

2.3.2 Wind and temperature profiles in the IBL

Vertical profiles of wind speed and temperature are assumed to be self-similar in the IBL, developing in the Ekman part of the PBL. Profiles for temperature $\theta(z)$ and wind speed $U(z)$ are written in the form

$$\theta(z,x) = \theta(\delta) + \mathcal{F}_\theta(\xi), \tag{67}$$

$$U(z,x) = G + \mathcal{F}_u(\xi), \tag{68}$$

where $\mathcal{F}_\theta(\xi)$ and $\mathcal{F}_u(\xi)$ are the similarity functions and

$$\xi = \frac{z-h}{\delta - h} \tag{69}$$

is the dimensionless vertical coordinate. Wind and temperature profiles explicitly depend on fetch, as the height of the IBL $\delta = \delta(x)$ depends on x.

Substituting (67), (68) into (58), (59) following equations for temperature and wind profiles in ξ-coordinate are obtained

$$\frac{\partial^2}{\partial \xi^2}\mathcal{F}_\theta(\xi) + 2\alpha\xi\frac{\partial}{\partial\xi}\mathcal{F}_\theta = \beta, \tag{70}$$

$$\frac{\partial^2}{\partial \xi^2}\mathcal{F}_u(\xi) + 2\alpha\xi\frac{\partial}{\partial\xi}\mathcal{F}_u - 2id^2\mathcal{F}_u = -2d^2U_T\left[\frac{\mathcal{F}'_\theta(\xi) - \mathcal{F}'_\theta(1)}{\mathcal{F}'_\theta(0)}\right], \tag{71}$$

where parameters α and β are

$$\alpha = \frac{\bar{u}}{4K}\frac{\partial}{\partial x}(\delta - h)^2 \tag{72}$$

and

$$\beta = 2\gamma_0(\delta - h)\alpha - \frac{(\delta-h)^2}{K}\bar{u}\frac{\partial}{\partial x}\Delta\theta. \tag{73}$$

The α parameter defines the growth rate of the IBL, while the β parameter defines the impact of the temperature gradient in the background atmosphere and of the temperature jump across the inversion on the structure of the IBL. The dimensionless height d is

$$d = \frac{\delta - h}{H}. \tag{74}$$

Deriving (71) we have neglected the vertical velocity gradient in the background atmosphere (at heights $z > \delta$, as it is small there.

The following boundary conditions are required. At the upper IBL boundary $z = \delta$ (or $\xi = 1$) due to (67) the temperature universal function is equal to zero:

$$\mathcal{F}_\theta(1) = 0. \tag{75}$$

Due to (68) the velocity universal function is

$$\mathcal{F}_u(1) = U(\delta) - G. \tag{76}$$

At the lower boundary of the Ekman part of the IBL, i.e. at $z = h$ ($\xi = 0$) momentum and heat fluxes are continuous and are equal to corresponding fluxes at the upper boundary of the SBL

$$\frac{\partial \mathcal{F}_\theta}{\partial \xi} = -\frac{q_s}{K}(\delta - h), \tag{77}$$

$$\frac{\partial \mathcal{F}_u}{\partial \xi} = \frac{\tau_s}{K}(\delta - h), \tag{78}$$

where $\tau_s = u_*^2 \exp(i\phi_s)$ and ϕ_s is the angle between the surface stress vector and the x axis.

Equation (70) is the classical equation of the heat conduction in a media with a constant exchange coefficient. Its first integral reads

$$\frac{\partial \mathcal{F}_\theta}{\partial \xi} = -\frac{q(\delta - h)}{K} e^{-\alpha\xi^2} + \beta e^{-\alpha\xi^2} \int_0^\xi e^{\alpha\xi^2} d\xi. \tag{79}$$

By integrating (79) with the boundary condition (75) the distribution of temperature can be obtained for known parameters α and β.

The general solution of equation (71) is

$$\mathcal{F}_u = \mathcal{F}_{u0} + \mathcal{F}_{us}, \tag{80}$$

where $\mathcal{F}_{u0}$ is the solution of the homogeneous equation and $\mathcal{F}_{us}$ is a partial solution of (71). A partial solution of eq. (71) has the form

$$\mathcal{F}_{us} = U_T \left\{ \frac{d^2}{\alpha + id^2} \frac{\mathcal{F}'_\theta(\xi)}{\mathcal{F}'_\theta(0)} + i \frac{\mathcal{F}'_\theta(1)}{\mathcal{F}'_\theta(0)} \right\}. \tag{81}$$

The exact solution $\mathcal{F}_{u0}$ of the homogeneous equation is not known. We shall search for an approximate solution of $\mathcal{F}_{u0}$ in the form

$$\mathcal{F}_{u0} = \sum_{i=0}^{n} c_i \xi^i. \tag{82}$$

Substituting (82) into (71) (with the r.h.s. equals 0) the solution of the homogeneous equation is obtained

$$\mathcal{F}_{u0}(\xi) = c_1(1 + id^2\xi^2) + c_2\xi(1 - \frac{1}{3}(\alpha - id^2)\xi^2) + O(\frac{1}{4!} \cdot \xi^4). \tag{83}$$

The partial solution (81) can be approximately rewritten in the form

$$\mathcal{F}_{us} = U_T \frac{d^2}{\alpha + id^2} \frac{\mathcal{F}'_\theta(\xi) - \mathcal{F}'_\theta(1)}{\mathcal{F}'_\theta(0)}. \tag{84}$$

When the thermal wind plays a role ($d^2 \sim 1$) eq. (81) and (84) are close to each other. At early stages of the IBL growth $d^2 \ll 1$ and equations diverge but baroclinicity effects at this stage are negligible.

The exact solution (79) for the temperature gradient can be rewritten in the approximate form similar to (82):

$$\frac{\partial \mathcal{F}_\theta}{\partial \xi} = -\frac{q_s}{K}(\delta - h)(1 - \alpha\xi^2) + \beta\xi(1 - \frac{2}{3}\alpha\xi^3). \tag{85}$$

Substituting (85) into (84) we obtain

$$\mathcal{F}_{us} = U_T \frac{d^2}{\alpha + id^2}\left[F_q(\xi) - F_q(1)\right], \tag{86}$$

where $F_q(\xi)$ is the universal function of the heat flux in the IBL defined by

$$q_\xi = q_s F_q(\xi) \tag{87}$$

with

$$F_q(\xi) = 1 - \alpha\xi^2 - \frac{\beta K}{q_s}\frac{1}{(\delta - h)}(\xi - \frac{2}{3}\alpha\xi^3). \tag{88}$$

The sum of solutions (83) and (86) gives the general solution for the wind profile. Constants c_1 and c_2 are chosen to satisfy the boundary conditions (76), (78):

$$c_1(1 + id^2) + c_2(1 - \frac{1}{3}(\alpha - id^2)) = U_\delta - G, \tag{89}$$

$$c_2 - U_T \frac{d^2}{\alpha + id^2}\frac{\beta K}{q_s(\delta - h)} = \frac{\tau_s}{K}(\delta - h). \tag{90}$$

Solving (89), (90) for c_1 and c_2 the solution for the wind profile is found

$$U - G = -2A(\mu)\frac{\vec{u}_*}{\kappa}F_u(\xi, \alpha, d) \cdot d + (U_\delta - G)\frac{1 + id^2\xi^2}{1 + id^2} + \mathcal{U}_T \tag{91}$$

with

$$\mathcal{U}_T(\xi) = U_T \frac{d^2}{\alpha + id^2}\left[F_q(\xi) - F_q(1) - \frac{1}{(\delta - h)}\frac{\beta K}{q_s}F_u(\xi, \alpha, d)\right], \tag{92}$$

where $\vec{u}_* = u_* \exp(i\phi_s)$ and F_u is a universal function of the wind profile

$$F_u(\xi, \alpha, d) = \frac{(1 - \xi)(1 - id^2\xi)}{1 + id^2} - \frac{1}{3}\frac{\alpha - id^2}{1 + id^2}\left(1 - \xi^3 + id^2\xi^2(1 - \xi)\right). \tag{93}$$

As before the universal function A is

$$A(\mu) = \frac{\kappa u_*}{Hf}. \tag{94}$$

The heat flux defines the universal distribution of temperature in the IBL. We use

$$q = -\frac{K}{(\delta - h)}\frac{\partial\theta}{\partial\xi} \tag{95}$$

to obtain the $\theta(\xi)$ profile which satisfies the boundary condition (75)

$$\theta(\xi) - \theta(1) = -2dA(\mu)\frac{\theta_*}{\kappa}F_\theta(\xi), \tag{96}$$

$$F_\theta(\xi) = \int_\xi^1 F_q(\xi)d\xi. \tag{97}$$

Equations (91), (96) and (87) describe the IBL structure. To obtain the solution we still need to define the growth rate parameter α and thus an equation for the IBL height growth. We also need to define heat and momentum fluxes at the lower boundary of the Ekman part of the IBL (which equal the fluxes at the top of the SBL) and thus to obtain the resistance laws of the IBL.

2.3.3 Evolution of the IBL: asymptotic regimes

a) Evolution of the thermal IBL in the near-neutral atmosphere. The temperature gradient above the IBL height is assumed to be zero, i.e. $\gamma_0 = 0$. It is reasonable to assume further, that in such conditions the IBL (both stably or unstably stratified) develops without the temperature jump across its upper boundary $\xi = 1$. In this case parameter $\beta \equiv 0$. To calculate the growth rate parameter α we additionally assume that the heat flux (temperature gradient) equals zero at $\xi = 1$. From (87) it follows $\alpha = 1$ and the equation of the IBL height growth takes the form

$$\bar{u}\frac{\partial}{\partial x}\delta^2 = 4K. \tag{98}$$

Universal functions of the heat flux and temperature are

$$F_q(\xi) = 1 - \alpha\xi^2, \tag{99}$$

$$F_\theta(\xi) = (1 - \frac{1}{3}\alpha) - \xi + \frac{1}{3}\alpha\xi^3 \tag{100}$$

(we keep here α-parameter, though for this particular case $\alpha = 1$).

b) IBL and the background atmosphere have the same type of stratification. We assume that the IBL develops without the temperature jump across its upper boundary $\Delta\theta = 0$. The β- parameter then equals

$$\beta = 2\gamma_0(\delta - h)\alpha. \tag{101}$$

To calculate the growth rate parameter α we additionally assume that the temperature gradient at $\xi = 1$ is equal to its background value γ_0. The heat flux at $\xi = 1$ is then $q(1) = -K\gamma_0$ and the equation for α follows from (87), (88):

$$\frac{4}{3}\frac{K\gamma_0}{q_s}\alpha^2 - \alpha(1 + 2\frac{K\gamma_0}{q_s}) + (1 + \alpha) = 0. \tag{102}$$

The solution of this equation is

$$\alpha = \frac{3}{8}(\frac{K\gamma_0}{q_s})^{-1}\left\{1 + 2\frac{K\gamma_0}{q_s} - \left[1 - \frac{4}{3}\frac{K\gamma_0}{q_s}(1 + \frac{K\gamma_0}{q_s})\right]^{1/2}\right\}. \tag{103}$$

Parameter $K\gamma_0/q_s$ varies in the range $-1 \le K\gamma_0/q_s \le 0$ so that the solution of (103) lies in the range $3/4 \le \alpha \le 1$. We shall neglect this variability of α and simply assume $\alpha = 1$. The equation of the IBL height growth takes the form (98) and universal functions of the heat flux and temperature are

$$F_q(\xi) = 1 - \alpha\xi^2 - 2\alpha\frac{K\gamma_0}{q_s}\xi(1 - \frac{1}{2}\alpha\xi^2), \tag{104}$$

$$F_\theta(\xi) = (1 - \frac{1}{3}\alpha) - \xi + \frac{1}{3}\alpha\xi^3 - \alpha\frac{K\gamma_0}{q_s}\left[1 - \xi^2 - \frac{1}{4}\alpha(1 - \xi^4)\right] \tag{105}$$

When $\gamma_0 \to 0$ (104), (105) asymptotically converge to (99), 100.

c) Stably stratified IBL in unstable atmosphere. In this case it is also reasonable to assume, that the IBL develops without the temperature jump across its upper boundary $\xi = 1$. The temperature gradient above the IBL is equal to 0. The growth rate parameter α then follows from (103). The temperature gradient in the background atmosphere is zero, i.e. $|\gamma_0 K/q_s| = 0$. (Hereafter we take the temperature gradient in the convective background atmosphere equals 0.) When $|\gamma_0 K/q_s| = 0$ the solution of (103) is $\alpha = 1$. The equation of the IBL height growth takes the form (98) and universal functions of the heat flux and temperature are equal to (104), (105).

d) Convective IBL in stably stratified atmosphere. It is well known (Garratt, 1991) that when convective IBL develops in stably stratified atmosphere the inversion temperature jump $\Delta\theta$ is formed at its lower boundary. This temperature jump is related to the

entrainment of a weakly turbulent warmer air of stable background atmosphere into strongly turbulent unstable IBL. The corresponding heat flux is

$$\Delta q \equiv q(\delta_{-0}) - q(\delta_{+0}) = -\Delta\theta\bar{u}\frac{\partial\delta}{\partial x}, \tag{106}$$

where $q(\delta_{-0}) \gg q(\delta_{+0})$. To model the evolution of the convective IBL it is important to account correctly for the heat flux $q(\delta_{-0})$. Garsen (1973), Tennekes (1973) take $q(\delta_{-0}) = c_e q_s$, where $c_e = 0.2$. We estimate the growth rate parameter α from the condition that the heat flux at its upper boundary is equal to the entrainment heat flux. From (87) and (106) at $\xi = 1$ follows equation for α

$$q_s\left[1 - \alpha - \left(2\frac{\gamma_0 K}{q_s}\alpha - \frac{\delta - h}{q_s}\bar{u}\frac{\partial}{\partial x}\Delta\theta\right)(1 - \frac{2}{3}\alpha)\right] = -\Delta\theta\bar{u}\frac{\partial\delta}{\partial x} - q_0, \tag{107}$$

where $q_0 = q(\delta_{+0})$. With the temperature jump across the inversion in the form (37) the equation (107) takes the form

$$\alpha^2(1-\epsilon) - \frac{3}{2}\alpha\left[(1-2\epsilon) + \frac{1}{2}\frac{\gamma_0 K}{q_s}\right] + \frac{3}{4}\frac{\gamma_0 K}{q_s}(1 - \frac{q_0}{q_s}) = 0. \tag{108}$$

The ϵ parameter varies in the range $0 \leq \epsilon \leq 0.5$. When $\epsilon = 0$ there is no temperature jump . When $\epsilon = 1/2$ the IBL growth takes place under intensive mixing but without heating from beneath. The temperature gradient in the well mixed convective IBL is much smaller than in the background atmosphere which means $q_s/(\gamma_0 K) \ll 1$. Two approximate solutions of equation (108) are

$$\alpha_1 \simeq \frac{1}{2(1-2\epsilon)}\frac{(q_s - q_0)}{K\gamma_0} + O\left((\frac{q_s}{K\gamma_0})^2\right), \tag{109}$$

$$\alpha_2 \simeq \frac{3}{2}\frac{1-2\epsilon}{1-\epsilon} + O(\frac{q_s}{K\gamma_0}). \tag{110}$$

The physical meaning has only the first solution (109) which gives the entrainment heat flux

$$q_\delta - q_0 = -\Delta\bar{u}\frac{\partial\delta}{\partial x} \equiv -\frac{\epsilon}{1-2\epsilon}(q_s - q_0). \tag{111}$$

The equation (111), when $q_0 \ll q_s$, corresponds to the relation for the entrainment heat flux of Tennekes (1973) model. To comply with his constant $c_e = 0.2$ we have to set $\epsilon = 0.15$. When ϵ is taken to be 0.25, relation (111) agrees with numerical model results of Ventkatram (1977).

From (109) and (72) the equation of the convective IBL height growth takes the form

$$\bar{u}\frac{\partial}{\partial x}\delta^2 = \frac{2}{1-2\epsilon}\frac{q_s - q_0}{\gamma_0}. \tag{112}$$

The equation (112) becomes invalid when $\gamma \to 0$. (Note, that this solution was obtained under the condition $q_s/(\gamma_0 K) \ll 1$). When $\gamma_0 \equiv 0$ the equation of the IBL growth has the form (98). We merge equations (98) and (112) to obtain the generalized equation of the IBL growth

$$\bar{u}\frac{\partial}{\partial x}\delta^2 = 4K\frac{1 - q_0/q_s}{1 + \gamma_0 K/q_s}, \tag{113}$$

where we took $\epsilon = 0.25$. When $\gamma_0 K/q_s \gg 1$ (113) converges to (98). When $\gamma_0 K/q_s \ll 1$ (113) converges to (112). For the growth of the convective IBL we shall further use the equation (113) and define the growth rate parameter as

$$\alpha = \frac{1 - q_0/q_s}{1 + \gamma_0 K/q_s}. \tag{114}$$

Universal functions of the heat flux and temperature are

$$F_q(\xi) = 1 - \alpha\xi^2 - 2\alpha\frac{K\gamma_0}{q_s}(1 - \epsilon)(\xi - \frac{1}{2}\alpha\xi^3), \tag{115}$$

$$F_\theta(\xi) = 1 - \xi - \frac{1}{3}\alpha(1 - \xi^3) - \frac{K\gamma_0}{q_s}\alpha(1 - \epsilon)\left[(1 - \xi^2) - \frac{1}{4}\alpha(1 - \xi^4)\right]. \tag{116}$$

When $q_s/(\gamma_0 K) \ll 1$ (or $\alpha \ll 1$) and $q_0/q_s \ll 1$ (115), (116) are simplified to

$$F_q(\xi) = 1 - \frac{3}{2}\xi, \tag{117}$$

$$F_\theta(\xi) = \frac{1}{4} - \xi + \frac{3}{4}\xi^2. \tag{118}$$

From (117) it follows, that the heat flux decreases linearly with height to a value of $-1/2q_s$ and is equal to the entrainment heat flux. The mean temperature of the IBL $\theta(\delta)$ is smaller than temperature of the background atmosphere on a value of $1/4\gamma_0\delta$. Note, that heating of the IBL while it develops can lead to $q_s = 0$. In this case the growth rate parameter $\alpha = K_0/K$.

e) Neutral IBL: transformation across an abrupt change in roughness. In this case the wind profile has the form (91) where $U_T = 0$. The universal function of the wind stress F_τ is defined by

$$\tau(\xi) = \tau_s F_\tau(\xi), \tag{119}$$

$$F_\tau = -\frac{\partial F_u}{\partial \xi} = 1 - \frac{2id^2}{1 + id^2}\xi - \frac{\alpha - id^2}{1 + id^2}\xi\left(\xi - id^2(\frac{2}{3} - \xi)\right). \tag{120}$$

When $\xi = 0$, $F_\tau(0) = 1$ and the stress is continuous across the lower boundary of the IBL (the upper boundary of the SBL). At the upper boundary $\xi = 1$ of the IBL

$$F_\tau(1) = \frac{1}{1 + id^2}\left(1 - \alpha - \frac{1}{3}d^2(d^2 + i\alpha)\right). \tag{121}$$

To calculate the growth rate parameter α we need as before an additional condition. We assume that the vertical shear of the wind velocity is zero at the upper boundary of the IBL. The equation to calculate α then follows

$$1 - \alpha - \frac{1}{3}d^2(d^2 + i\alpha) = 0. \tag{122}$$

When the IBL is fully developed ($\alpha \equiv 0$) it follows from (122) that $d^{1/4}_{\max} = 3$. Using $\varepsilon = h/H = 0.15$ we obtain $\delta_{\max} \simeq 1.5H$. This estimate agrees well with the traditional estimate of the height of the equilibrium IBL $\delta_{\max} \simeq 0.2u_*/f$.

On early stages of the IBL growth $d^2 \ll 1$. From (122) $\alpha \simeq 1$ and the equation of the neutral IBL growth corresponds to (46), where K is taken at its neutral value. On a stage close to a fully developed IBL $d^2 \gg \alpha$ and from (122)

$$\alpha \simeq 1 - \frac{1}{3}d^4. \tag{123}$$

The height of the IBL is bounded by the value $d^{1/4}_{\max} = 3$, so the equation (123) describes the IBL growth towards the equilibrium state. From physical point of view the growth of the IBL is limited by the balance of the TKE production due to the wind shear and its dissipation. The concept of the IBL implies that there is no turbulence when $z > \delta_{\max}$, or formally $K = 0$. We rewrite equation (123) in the form

$$\alpha \simeq 1 - (\frac{\delta}{D})^4, \tag{124}$$

where $D = \delta_{\max}$ is the height of the equilibrium PBL. This height can be expressed via the PBL scale H as

$$D = mH = m\frac{\kappa u_*}{f}\frac{1}{A(\mu)}, \tag{125}$$

where $m \simeq 3^{1/4} + \varepsilon$.

2.3.4 Evolution of the IBL: generalization

For the generalized description of the mesoscale evolution of the IBL we shall merge special solutions, obtained in the previous subsection, into one equation. This is the so called 'interpolation' approach. The generalized equation has to have the correct asymptotic solutions when the dimensionless parameters of the equation approach their limits.

Growth of the IBL. The generalized equation of the mesoscale IBL height growth is taken in the form

$$\bar{u}\frac{\partial}{\partial x}\delta^2 = 4\alpha K(h), \tag{126}$$

where $K(h)$ is the eddy-viscosity coefficient at the upper boundary of the SBL, and the growth rate parameter α

$$\alpha = \alpha_\gamma \left[1 - (\frac{\delta}{D})^4\right], \tag{127}$$

$$\alpha_\gamma = \frac{1 + \max(\gamma_0 K_0/q_s, 0)}{1 + \max(\gamma_0 K/q_s, 0)}. \tag{128}$$

The growth of the IBL according to (127) is limited by the height of the equilibrium PBL when $\delta \to D$. This limit appears in the description of the neutral IBL growth. However the growth of the thermal IBL should also be limited: when $\delta \to D$ the TKE production due to the wind shear and buoyancy is balanced by its dissipation. In (127), (128) α_γ accounts for the stratification of the background atmosphere. The relation for α_γ corresponds to the relation (46) obtained for the growth of the convective IBL in the SBL. It has the following asymptotic regimes

- when $\gamma_0 \simeq 0$ (the background atmosphere is unstable or near-neutral) then $\alpha_\gamma = 1$. The growth rate parameter corresponds to regimes described in a), c) and e);
- if stably stratified IBL develops in stable atmosphere then $\alpha_\gamma = 1$. This corresponds to the regime described in b);
- if the convective IBL develops in stably stratified atmosphere then $\alpha_\gamma \simeq q_s/(\gamma_0 K)$ which correspond to the regime described in d).

Equation (126) describes the mesoscale evolution of the IBL. If we compare it with the equation (44), which describes the small scale growth of the IBL, we can notice, that (44) will converge to (126) when δ will exceed the equilibrium height of the SBL. Equation (126) appears to describe uniformly the evolution of the IBL on both small scales and mesoscales, unless the new PBL is fully adjusted to the new surface.

Wind and temperature profiles in the IBL. Generalized equations describing wind, temperature and heat flux profiles in the IBL have the form:

wind profile:

$$U - G = -2A(\mu)\frac{\vec{u}_*}{\kappa} \cdot d \cdot F_u(\xi) + (U_\delta - G)\frac{1 + id^2\xi^2}{1 + id^2} + \mathcal{U}_{Tg} \tag{129}$$

with

$$\mathcal{U}_{Tg}(\xi) = U_T \frac{d^2}{\alpha + id^2} \left[F_q(\xi) - F_q(1) - 2\alpha(1-\epsilon_\theta)\frac{\gamma_0 K}{q_s} F_u(\xi) \right]; \tag{130}$$

temperature profile:

$$\theta(\xi) - \theta(1) = -2dA(\mu)\frac{\theta_*}{\kappa} F_\theta(\xi); \tag{131}$$

heat profile:

$$q(\xi) = q_s F_q(\xi). \tag{132}$$

The universal function F_u is

$$F_u(\xi) = \frac{(1-\xi)(1-id^2\xi)}{1+id^2} - \frac{1}{3}\left(\frac{\alpha - 0.75id^2}{1+id^2}\right)\left(1 - \xi^3 + id^2\xi^2(1-\xi)\right) \tag{133}$$

(coefficient 0.75 is introduced here for a better agreement with observations in a case when the IBL is fully developed $\alpha \to 0$).

Universal functions for the heat flux and temperature F_θ and F_q are

$$F_q(\xi) = (1 - \alpha\xi^2) - 2\alpha\frac{\gamma_0 K}{q_s}(1-\epsilon_\theta)(\xi - \frac{1}{2}\alpha\xi^3), \tag{134}$$

$$F_\theta(\xi) = (1-\xi) - \frac{1}{3}\alpha(1-\xi^3) - \frac{\gamma_0 K}{q}\alpha(1-\epsilon_\theta)\left[(1-\xi^2) - \frac{1}{4}\alpha(1-\xi^4)\right]. \tag{135}$$

Equations (131) and (135) have to be considered with the possible temperature jump across the inversion at the top of the convective IBL

$$\theta(\delta) = \theta_0(\delta) - \epsilon_\theta\gamma_0\delta, \tag{136}$$

where $\epsilon_\theta = \max(0, 0.25\mathrm{sign}q_s)$. The convective IBL in the process of its development can become neutral or even stable. To allow for the smooth transition through the point where $q = 0$ we define ϵ_θ in the form

$$\epsilon_\theta = \max\left(0, \frac{1}{4}\frac{q_s}{\gamma_0 K}\frac{1}{\alpha_\gamma}\right). \tag{137}$$

In the convective IBL $|q_s/\gamma_0 K| \ll 1$ and $\alpha_\gamma = \gamma_0 K/q_s$ (see eq. (128)). Parameter ϵ_θ equals then 0.25 and the temperature jump is well pronounced. When the convective IBL collapses $q_s \to 0$, $\epsilon_\theta \to 0$ and the temperature jump smoothly diminishes.

Note, that the universal profile functions depend on the growth rate parameter α. In latest stages of the IBL evolution when $\alpha \to 0$ (or $\delta \to D$) profile functions describe the structure of the equilibrium PBL. The baroclinicity term (second term on the r.h.s. of (129)) which appears in the wind profile is directly proportional to α. That is why the thermal wind can exist only when the IBL develops. When a stage of development is close to equilibrium the thermal wind disappears.

Resistance laws. The resistance laws are obtained by overlapping profiles of temperature and wind velocity in the SBL and the Ekman part of the IBL at height $z = h$ (or $\xi = 0$). The velocity resistance law is

$$\frac{\vec{u}_*}{\kappa}\left[\ln(\frac{h}{z_0}) - \Psi_u(h/L)\right] = G - 2A(\mu)\frac{\vec{u}_*}{\kappa}\cdot d\cdot F_u(0) + (U_\delta - G)\frac{1}{1+id^2} + \mathcal{U}_T(0), \qquad (138)$$

where

$$\mathcal{U}_T(0) = U_T\frac{d^2}{\alpha + id^2}\left[F_q(0) - F_q(1) - 2\alpha(1-\epsilon_\theta)\frac{\gamma_0 K}{q_s}F_u(0)\right]. \qquad (139)$$

The temperature resistance law is

$$\theta_s + \frac{\theta_*}{\kappa}\left[\ln(\frac{h}{z_{0t}}) - \Psi_\theta(h/L)\right] = \theta(\delta) - 2dA(\mu)\frac{\theta_*}{\kappa}F_\theta(0). \qquad (140)$$

Taken into account that $h = \varepsilon H$ the resistance laws (138) and (140) can be rewritten in a 'common' form

$$\frac{\kappa G}{\vec{u}_*}\left[1 + (\frac{U_\delta}{G} - 1)(1+id^2)^{-1}\right] = \ln(\frac{\kappa u_*}{f z_0}) - B(\mu, d) + F(\mu, d), \qquad (141)$$

$$\frac{\kappa(\theta_\delta - \theta_s)}{\theta_*} = \ln(\frac{\kappa u_*}{f z_{0t}}) - C(\mu, d), \qquad (142)$$

where $\mu = \kappa u_*/fL$ is the stratification parameter, C, B are universal functions and F is the baroclinicity function:

$$C(\mu, d) = -2dA(\mu)F_\theta(0) + \Psi_\theta(\varepsilon\mu/A) - \ln(\frac{\varepsilon}{A}), \qquad (143)$$

$$B(\mu, d) = -2dA(\mu)F_u(0) + \Psi_u(\varepsilon\mu/A) - \ln(\frac{\varepsilon}{A}), \qquad (144)$$

$$F(\mu, d) = i\frac{\kappa}{\vec{u}_*}\frac{\beta}{f\bar{u}}\cdot\frac{d^2}{d^2 - i\alpha}q_s\left[F_q(0) - F_q(1) - 2\alpha(1-\epsilon_\theta)\frac{\gamma_0 K}{q_s}F_u(0)\right]. \qquad (145)$$

Equations (141) and (142) are solved for $\vec{u_*}$ and θ_* for the dimensionless IBL height $d = (\delta - h)/H$. When $d = 0$ the resistance laws of the IBL converge to the resistance laws of the SBL (see eq.(52)). When the height of the IBL approaches the height of the equilibrium PBL the growth rate parameter $\alpha \to 0$ and (141), (142) correspond to the resistance laws of the equilibrium PBL.

2.4 Description of the model

The equations obtained in sections 2.2.3, 2.2.4 and 2.3.4 uniformly describe the PBL transformation caused by an abrupt change in surface temperature or/and surface roughness across a coastal line, on both small scales and mesoscales. The similarity approach (the IBL structure depends on fetch implicitly) gives the possibility to solve effectively the model equations. The local IBL structure is calculated for each of the dimensionless IBL heights. Then the solution for every IBL height is related to the spatial coordinates. For that the equation of the IBL growth rate is used.

2.4.1 External parameters of the model

The external parameters of the model which have to be defined are:

- geostrophic wind speed and its direction $\vec{G}$;
- temperature of the air at any relatively high level (of order 1000m) θ_a;
- land θ_l and sea θ_s surface temperature;
- land roughness z_0.

The only tuning parameter of the model is ε, taken to be 0.1. The height of the equilibrium PBL $D = mH$ is defined by the m-parameter which equals 1.5 (see section 2.3.3).

2.4.2 Structure of the background PBL

To initialize the model the structure of the upwind background (undisturbed) PBL is to be determined. It depends on the external parameters.

- The background friction velocity u_{*b}, the surface wind speed direction ϕ_{sb} and the temperature scale θ_{*b} are determined from the resistance laws (141) and (142), where the growth rate parameter $\alpha = 0$ and the dimensionless height $d = m - \varepsilon = (D-h)/H$.
- Heights of the PBL and the SBL are calculated from (125) and (4).
- Wind and temperature profiles in the SBL are obtained from equations (47) and (48), and in the Ekman part of the PBL - from equations (129) and (131). Again $\alpha = 0$ and $d = m - \varepsilon$.

The description of the background atmosphere is hereby completed.

2.4.3 IBL structure

The IBL develops in the background atmosphere. The required input parameters are:

- an array of the dimensionless IBL depths $\tilde{\delta} = \delta/H$, $(d = \tilde{\delta} - \varepsilon)$;

- the external parameters mentioned in section 2.4.1;
- the known parameters of the background atmosphere (section 2.4.2).

The IBL structure is calculated as follows:

1. The local value of the friction velocity, the surface wind direction and the temperature scale are obtained from equations (52) and (53), if $\tilde{\delta} < \varepsilon$ (small scale evolution), or from equations (141) and (142), if $\varepsilon < \tilde{\delta} < m$ (mesoscale evolution). In the latter case the growth rate parameter α is defined by (127), (128).
2. The local SBL height is calculated from eq. (4) and (3) and the local IBL depth is defined by $\tilde{\delta}$ and the PBL scale H: $\delta = \tilde{\delta}H$.
3. Wind and temperature profiles in the SBL follow from (47) and (48), and in the Ekman part of the IBL - from (129) and (131). The growth rate parameter α is defined by (127), (128). In the case of the convective IBL the temperature inversion at the top of the IBL has to be taken into account by relations (136) and (137).

After the local structure of the IBL is obtained for each of the dimensionless IBL depths we need to map the solution on the spatial coordinates.

2.4.4 IBL as a function of fetch

To map the IBL solution on the x-coordinate we have to find the relation: $x = x(\tilde{\delta})$. That can be done using equations (44) and (126) for the IBL growth rate. These equations determine x as a function of the known parameters of the IBL:

$$\tilde{x} = \int_{\max(z_0, z_{0b})}^{D} p^{-1} \frac{\bar{u}}{G} \frac{\tilde{\delta}}{\alpha(d)} \frac{A(p\mu)}{A(\mu)} \frac{1}{H} d\delta, \tag{146}$$

where $p = \min(\tilde{\delta}/\varepsilon, 1)$ and the universal A function is defined by eq. (3). Here $\tilde{x} = xf/|G|$ is the dimensionless x-coordinate which is perpendicular to the coastal line. The dimensionless fetch (along the surface wind) is calculated from $\tilde{X} = \tilde{x}/\cos\phi_s$.

After the local IBL solutions are related to the spatial coordinates, the complete description of the PBL transformation in the coastal zone is achieved.

3 Model calculation: comparison with observations

In this section we shall verify the model. We shall perform some calculations and compare them with available observations. In section 3.1 the background PBL module is verified. Modelled IBL heights are compared with observations in section 3.2. Comparison of modelled and observed surface wind speed and temperature distributions along fetch is presented in section 3.3. For that we performed numerical simulations of two experiments: the NIBWAK and the Øresund experiment.

3.1 Background PBL

3.1.1 Tuning parameter

The model contains a single tuning parameter ε. Brown (1982) has estimated $\varepsilon \sim 0.1$. As our model differs in details from the original of (Brown, 982), we need to tune ε. For that we shall compare the asymptotic behaviour of the model PBL parameters (such as the PBL height D and the angle between the surface and the geostrophic wind $\Delta\alpha = \phi_s - \phi_g$) with well defined empirical relations presented e.g. in Zilitinkevich (1989a, 1989b).

The empirical asymptotic dependence of the PBL height and $\Delta\alpha$ in terms of the universal functions $\Lambda(\mu) = Df/u_*$ and $\sin\Delta\alpha = \mathcal{A}(\mu)u_*/\kappa|G|$ as a function of the stratification parameter μ has the form:

$$\Lambda_e(\mu) = \begin{cases} 0.3, & \text{if } \mu = 0 \\ \kappa\mu^{-1/2}, & \text{if } \mu \gg 1 \end{cases} \tag{147}$$

for the PBL height and

$$\mathcal{A}_e(\mu) = \begin{cases} 4.5 & \text{if } \mu = 0 \\ 1.8\mu^{1/2}, & \text{if } \mu \gg 1 \end{cases} \tag{148}$$

for the wind angle.

The model estimation for Λ and $\mathcal{A}$ functions follows from (125), (94), (2) and from (141), (144). The following relations are obtained:

$$\Lambda_m(\mu) = \begin{cases} 2m\kappa\varepsilon, & \text{if } \mu = 0 \\ (2/5)^{1/2}m\kappa\mu^{-1/2}, & \text{if } \mu \gg 1 \end{cases} \tag{149}$$

and

$$\mathcal{A}_m(\mu) = \begin{cases} \frac{3}{4\varepsilon}\frac{d_m^3}{1+d_m^4}, & \text{if } \mu = 0 \\ 2.37\frac{d_m^3}{1+d_m^4}\mu^{1/2}, & \text{if } \mu \gg 1 \end{cases} \tag{150}$$

In relation (149), the parameter m defines the PBL height via the scale H ($m = D/H$), and as has been shown in section 2.3.3 it should be close to $3^{1/4} + \varepsilon$. Tuning ε we find that a reasonable agreement between the model and the empirical asymptotic relations of Zilitinkevich is reached if we take $\varepsilon = 0.1$ and $m = 1.5$. In this case the model asymptotic for the Λ-function becomes

$$\Lambda_m(\mu) = \begin{cases} 0.12, & \text{if } \mu = 0 \\ 0.94\kappa\mu^{-1/2}, & \text{if } \mu \gg 1 \end{cases} \tag{151}$$

and for the $\mathcal{A}$-function

$$\mathcal{A}_m(\mu) = \begin{cases} 4.2 & \text{if } \mu = 0 \\ 1.34\mu^{1/2}, & \text{if } \mu \gg 1 \end{cases} \tag{152}$$

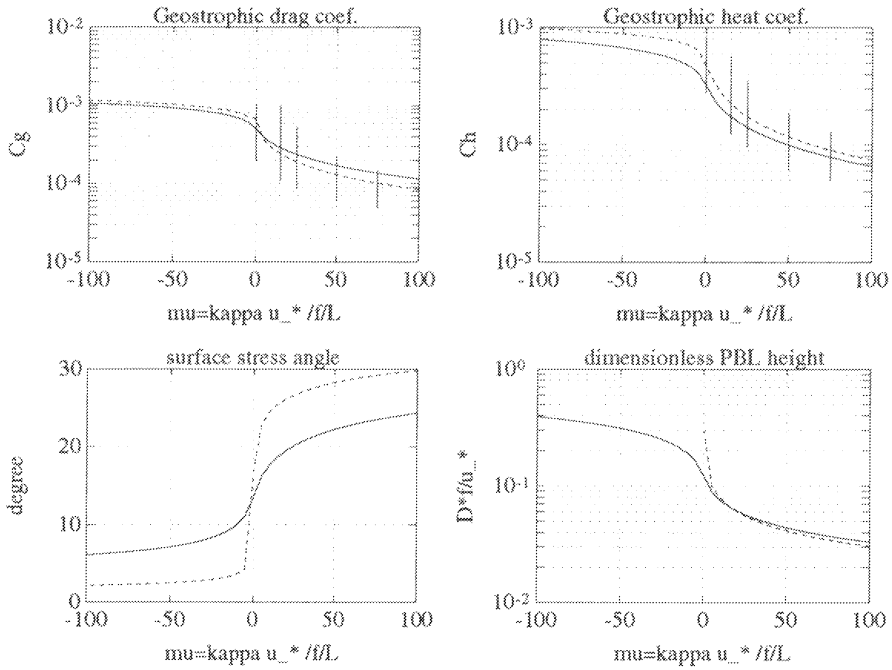

Figure 1: Geostrophic transfer coefficients of momentum C_g and heat C_h (two upper plots), the angle between the surface and geostrophic wind $\Delta\alpha$ and the dimensionless PBL height Df/u_* versus the stratification parameter $\mu = \kappa u_*/(fL)$. Full lines - model results. Dashed lines - semi-empirical relations of Zilitinkevich (1989a,1989b). Bars indicate the scatter in empirical estimates.

3.1.2 Geostrophic transfer laws

Model results are presented in figure 1 for the geostrophic transfer coefficient of momentum $C_g = (u_*/G)^2$ and heat $C_h = C_g^{1/2}\theta_*/(\theta_D - \theta_s)$, the dimensionless PBL height Df/U_*, and the angle between the geostrophic and the surface wind $\Delta\alpha = \phi_s - \phi_g$ as a function of the stratification parameter $\mu = \kappa u_*/(fL)$. Dashed lines are the semi-empirical relations which were proposed by Zilitinkevich (1989a, 1989b) for the neutral and the stably stratified PBL and by Zilitinkevich (1970) for the unstable atmosphere. Bars in the two upper plots indicate the range of the transfer coefficients which correspond to the scatter in the measured universal functions A, B, C (Zilitinkevich, 1989a, 1989b). Model results are consistent with empirical estimates, give the correct dependence of the PBL parameters on the stratification parameter and are in agreement with semi-empirical relations of Zilitinkevich.

In the study of the wind transformation on an abrupt change in surface roughness, it is important to check the correct dependence of the PBL parameters on the dimensionless surface roughness (Rossby number). In figure 2 the square root of the geostrophic transfer coefficient $C_g^{1/2}$ and the angle between the geostrophic and the surface wind are shown versus the Rossby number $Ro = G/(fz_0)$. Bars indicate the scatter of data which are taken from Zilitinkevich (1989a). The model results agree well with observations and show

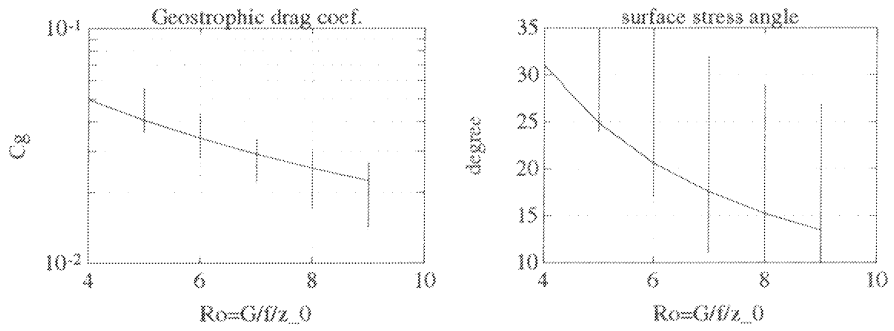

Figure 2: Geostrophic transfer coefficient of momentum $C_g^{1/2}$ and the angle between the surface and geostrophic wind $\Delta\alpha$ versus the Rossby number $Ro = G/(fz_0)$. Full lines - model results. Bars indicate the scatter in data (Zilitinkevich 1989a).

a qualitatively correct dependence of the geostrophic transfer coefficient and the direction of the surface wind on the Rossby number.

3.2 IBL height

3.2.1 Small scale evolution

The small scale IBL evolution takes place on fetch scales of a few kilometres. We recall the reader that the full adjustment of the PBL to a new surface takes place on a typical scale of 100 km. So, the small scale evolution of the IBL is the initial stage of the PBL transformation. However, this is an important stage of the IBL growth as it happens in the very vicinity of a coastal line. It is not surprising that this regime has been intensively studied in the laboratory and in the field. The form of equation (44), which describes the small scale IBL growth, has been chosen to agree the model results with observations. In this sense it is already validated against data. However we shall present a comparison of the model prediction of the IBL height h with field observations of Bergstrom et al. (1988), which were done under well controlled conditions.

In figure 3, taken from (Bergstrom et al., 1988), measured values of the IBL height are shown versus the stratification parameter z/L. The data were obtained over land at a distance of 1500m from a coastal line. The IBL was developing under a joint action of an abrupt change in the surface roughness and temperature. Its height varies from 20m in a

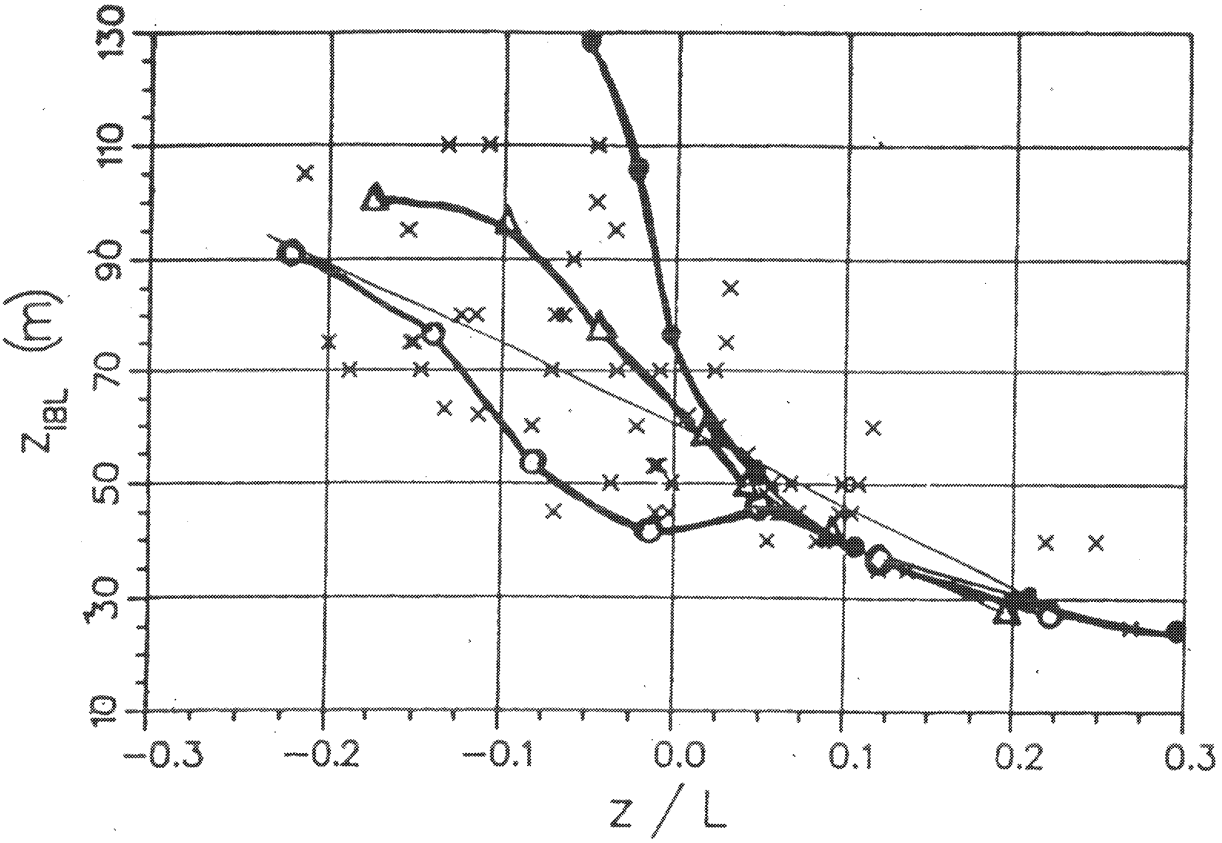

Figure 3: The measured heights (marks 'x') of the IBL over the land (1500 m from a coastal line) versus stability parameter z_{11}/L_l. The line is a linear regression $h = 61 - 141 z_{11}/L_l$. Compiled from Bergstrom et al. (1988). Model results are for the three states of the background atmosphere (over the sea). Open circles - neutral, $z_{11}/L_{sea} = 0$; triangles - stable, $z_{11}/L_{sea} = 0.05$; full circles - stable, $z_{11}/L_{sea} = 0.1$.

stable atmosphere to 110m in an unstable atmosphere. The calculated values of the IBL height resulting from equation (44) are also plotted. The model curves are for the three states of the background atmosphere (onshore wind) characterized by the stratification parameter z_{11}/L_{sea}, where $z_{11} = 11$m. They correspond to the neutral and a slightly stratified stable atmosphere: the stratification parameter z_{11}/L_{sea} over sea is 0, 0.05 and 0.1 respectively. When land is relatively cold ($z_{11}/L_l > 0$, stable stratification over the land) all curves converge and reproduce the measurements well. When land is relatively warm ($z/L_l < 0$, unstable stratification over the land) the model curves diverge. That is explained by the fact that the growth of the convective IBL depends sensitively on the stratification of the background atmosphere. The more stable is the background atmosphere, the less is the IBL growth (height) over the land. The important result is that the model explains the large scatter of data for unstable conditions over land. The model results of the small scale IBL growth are consistent with observations in a wide range of land-air temperature difference.

3.2.2 Mesoscale evolution

Convective IBL. A comprehensive review of experimental studies of convective IBL growth can be found e.g. in (Garratt, 1990). The wind-tunnel study of Meroney et al. (1975) shows a square root dependence of the IBL height on fetch. Raynor et al.(1975, 1979) used dimensional analysis and obtained a relation which approximates closely the observed IBL heights:

$$\delta = C_D^{1/2}\gamma_0^{-1/2}(\theta_l - \theta_s)^{1/2}X^{1/2}, \tag{153}$$

where $\theta_l - \theta_s$ is the temperature difference between the land and the sea. The empirical relation (153) is valid for fetches ranging from several km to about 50 km. In section 2.3.3 we have obtained the relation (eq. (113)) for convective IBL growth. The approximate solution of (113) for small fetches is (see eq. (42)):

$$\delta = 2C_H^{1/2}\gamma_0^{-1/2}(\theta_l - \theta_s)^{1/2}X^{1/2}, \tag{154}$$

where we used $\epsilon = 0.25$ and $q_s = C_H G(\theta_l - \theta_s)$. Equation (154) has the same form as (153). The difference in the proportionality coefficient results from the fact that we use the heat transfer coefficient instead of the drag coefficient to obtain the relation. Note that our relation agrees with the one of Venkatram (1977) obtained from the analysis of numerical calculations.

Stable thermal IBL. The field observation of stably stratified IBL growth has received increased attention in recent years. The growth of the stable thermal IBL was studied by e.g., Mulhearn (1981), Garratt (1987), Garratt and Ryan (1989). It was found that the IBL growth on fetches up to hundreds of km is relatively small (the IBL depth does not exceed the height of about 100m), and the IBL height obeys a square root dependence on X.

Mulhearn (1981) has analyzed measurements of temperature and the wind speed made in the offshore flow over the Massachusetts Bay. Using the dimensional analysis he suggested a relation which approximates well the observations:

$$\delta = 0.015u(g\Delta\theta/\theta)^{-1/2}X^{1/2}, \tag{155}$$

where $\Delta\theta$ is the temperature difference between the sea surface and the upstream flow. The same relation is obtained by Garratt (1987) who parameterized the results of numerical calculations.

In order to compare the model predictions of the IBL depth (equation (126)) with the empirical relation (155) we shall take into account the main features of the stably stratified IBL. Assuming that the IBL stratification is rather strong we prescribe that $\gamma_0 K/q_s \gg 1$. The IBL eddy-viscosity coefficient approximately equals

$$K = \frac{1}{5}\kappa u_* L. \tag{156}$$

Taking into account this relation, the solution of the equation (126) can be written as:

$$\delta = C[\frac{g}{\overline{T}}(\theta_{s0} - \theta_s)]^{-1/2}GX^{1/2}, \tag{157}$$

where constant C is: $C = [4C_D^2/(5C_H)]^{1/2}$. The model relation has the same form as the empirical one. For the stable IBL the transfer coefficients C_D and C_H are of about 10^{-4} which gives $C \sim 0.02$. That is in a good agreement with the empirical value 0.015 of equation (155). We conclude that the model results are consistent with field observations of the stably stratified IBL height.

Resuming this section we emphasize that equation (126) reasonably reproduces the known empirical data of the IBL growth for the arbitrary stratification and fetch scales.

3.3 Spatial variations of the surface wind and temperature: comparison with observations

3.3.1 The NIBWAK experiment

The experiment was performed in the period from July 28 to August 28, 1984 at the Nasudden peninsula on the island of Gotland in the Baltic Sea. The aim of the NIBWAK experiment was to study the IBL growth and the wind speed modification for air flow blowing from the sea into the land. Results of this experiment are published in Bergstrom et al. (1988). In section 3.2.1 we used the results of the NIBWAK experiment for the IBL height to verify the model. A good agreement of model results with measurements was found. In this section we shall try to reproduce modifications of the wind profile resulting from the transformation of the IBL along the fetch over land.

Measurements of the wind speed were made at levels $z = 3, 5, 10, 25m$ on several stations along the fetch (into the land). Data which are presented in figures 4, 5 and 9 of Bergstrom et al.(1988) are compiled here in figure 4 for unstable and in figure 5 for stable stratification above land. The observations show that in both cases the wind speed significantly drops as the air flow crosses the coastal line. This is due to the effect of the land roughness, which is larger than the roughness of the sea. The model results are performed for a neutral background atmosphere and a sea-land temperature difference of 2.5^o for the night time and -10^o for the day time. The model results are in reasonable agreement with the observations. They reproduce quantitatively the decrease of wind speed over land. Note, that in an unstable atmosphere the wind speed drops due to the effect of roughness and further increases with fetch due to the influence of unstable stratification.

3.3.2 The ØRESUND experiment

The experiment was performed in May - June 1984 to study the wind and temperature fields and the atmospheric dispersion over a region with cold water and warm land. Results of the ØRESUND experiment are reported in Gryning (1985), Doran and Gryning (1987), and Gryning and Joffre (1987). The east winds were blowing from Sweden over the Øresund strait into the main land of Denmark in the area close to Copenhagen. Measurements of wind speed and temperature were made at several stations over land and the strait.

Measurements of wind speed and air temperature at 10m height and of wind speed at 100m height along the line: the Swedish coast (the surface land temperature $\theta_l = 27^oC$, roughness $z_0 = 0.05$) - the strait (the water temperature $\theta_s = 12^oC$,) - the Danish coast

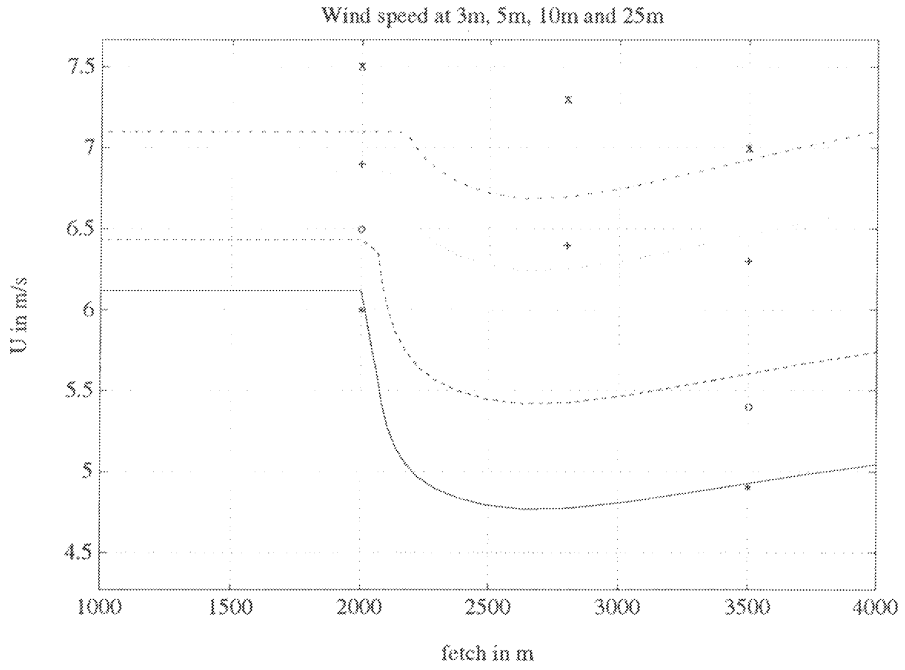

Figure 4: The wind profile along fetch over the land. Lines are model calculations, marks are measurements. Heights are: 3m (full line and stars '*'); 5m (dashed line and open circles 'o'); 10 m (dotted line and crosses '+'); 25m (dashed-dotted line and crosses 'x'). The coastal line is at fetch 2000m. Stratification over land is unstable.

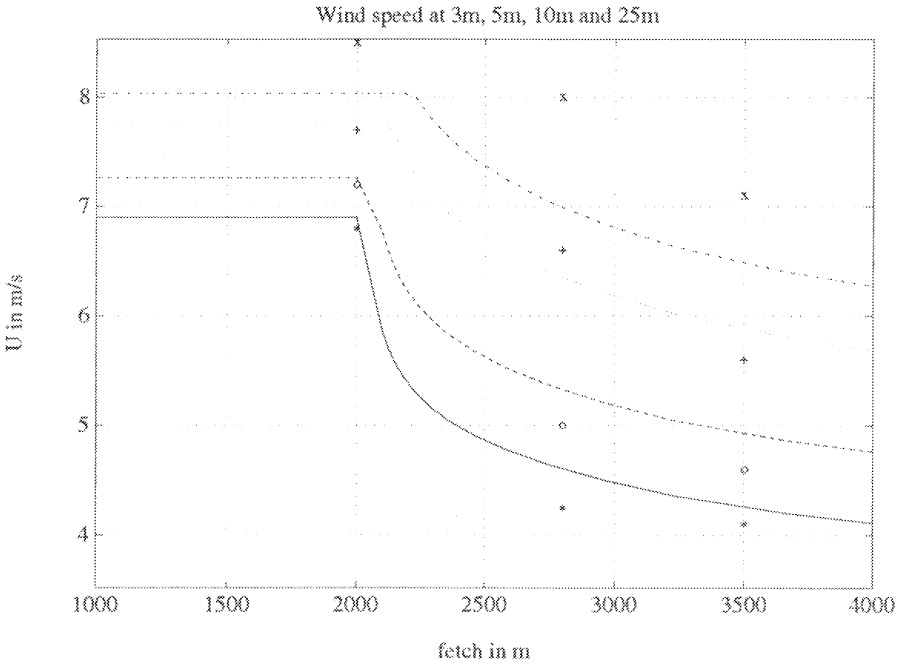

Figure 5: The same as in figure 4. Stratification over land is stable.

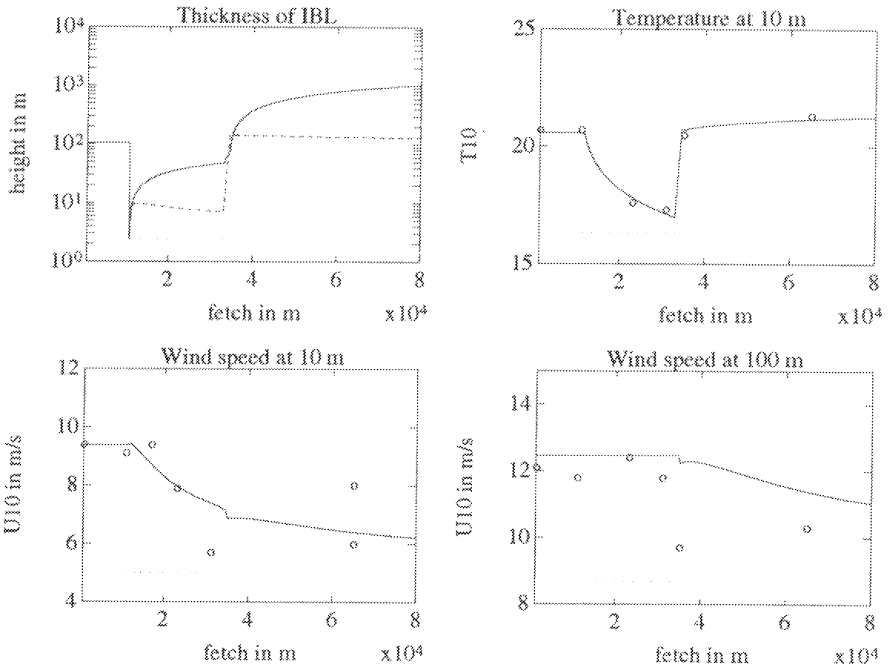

Figure 6: Measurements (open circles 'o') and model results (full and dashed lines) for the ØRESUND experiment. Upper left plot: solid line - the height of the IBL, dashed line - the height of the SBL. Upper right: temperature at 10 m height. Low left: wind speed at 10 m height. Low right - wind speed at 100m height. Dotted line indicates the Øresund strait.

($\theta_l = 27^oC$, $z_0 = 0.8$) are shown in figure 6. The background PBL over the Sweden coast correspond to a fetch 0-1km. The strait is shown by the dotted line. The characteristic features of the data reflect the interplay of two mechanisms. The warm air runs into cold water and decelerates due to the stably stratified conditions over the water. On the other hand it has a tendency to accelerate due to the effect of roughness: the water surface is much smoother than the land surface. From the data it is clear that the former mechanism is dominant - the wind speed reduces sharply when the air flow runs onto the water surface. When the air flow runs from cold water onto warm and very rough land the roughness effect dominates. The large roughness decelerates further the air flow, while the unstable conditions over the land tend to accelerate the flow. The decrease of the wind speed over the land is very marginal, which means that both mechanisms almost counteract each other.

Unlike the surface wind, the wind at 100m height does not show any deceleration of the flow over the strait which means that the disturbances in the PBL induced by the water surface are located below this height. However, the wind decelerates over the coast of Denmark because the disturbances in the PBL, caused by interaction of the air flow with the rough land, attain the 100m level. The model results for air temperature are in a good agreement with the data. The model wind speeds at 10m height quantitatively reproduce the observations. The model results of the wind speed reduction are consistent with observations even at a distance of about 70 km. The model also reproduces the decrease

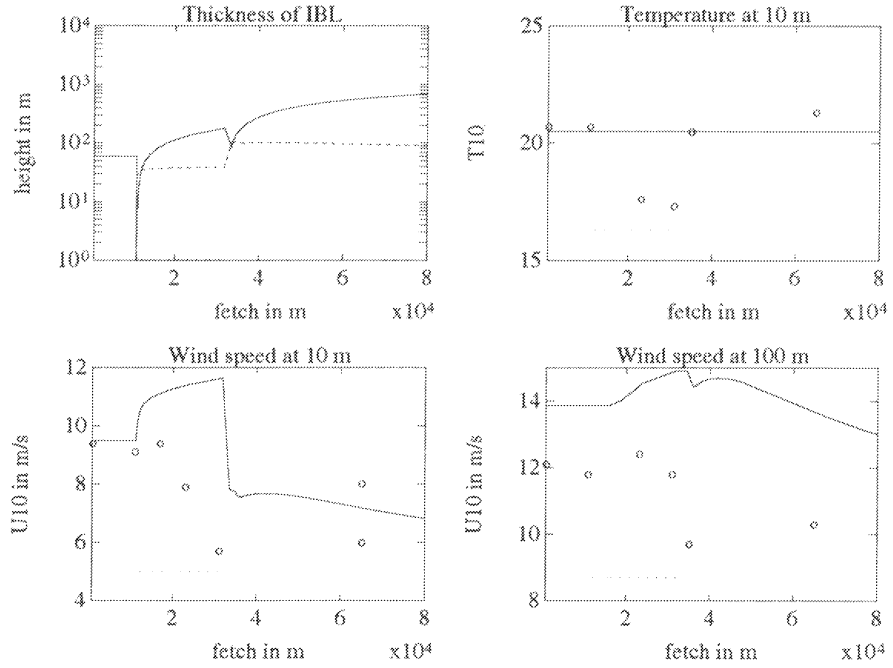

Figure 7: The same as in figure 6. Stratification effects are not accounted for in the model calculations.

in the wind speed at 100m height over the Danish coast, though it is not so pronounced as the measured one. The distribution of the IBL height (upper left plot) clearly shows that this decrease occurs as the IBL height exceeds the level of 100m. It also explains why the wind speed remains undisturbed over the strait at 100m height: the height of the IBL, where disturbances induced by the water surface are confined, is less than 100m.

To clarify the effect of stratification on the evolution of the IBL we perform a model experiment, where only the effect in roughness changes on the growth of the IBL is accounted for in the model. A neutral atmosphere is thus assumed over sea and land. Results are shown in figure (7). The temperature distribution is now uniform along the fetch. As is expected, the wind speed at 10 m height accelerates on a smooth water surface and then drops meeting a rough land surface. So, the drop of the wind velocity over the water observed in the Øresund experiment is due to a strong effect of the stratification and can not be reproduced by changes in roughness only. The depth of the IBL increases faster in the neutral atmosphere (upper left plot) and penetrates the 100m height over the strait. That results in an increase of the 100m wind speed over the strait, which is absent in the original simulation of the experiment. From this model experiment it is clear that models which describe the growth of the IBL on changes in roughness only, will fail to reproduce the observed structure of the IBL when the change in temperature across a coastal line is large enough.

In figure (8) the ratio between the wind speed over the water and the upwind wind over the land U_{10}/U_{10}^0, and the ratio between the temperature difference "air over water -water" and the temperature difference "upwind air over the land - water" $(\theta_{10} - \theta_s)/(\theta_{10}^0 - \theta_s)$ as

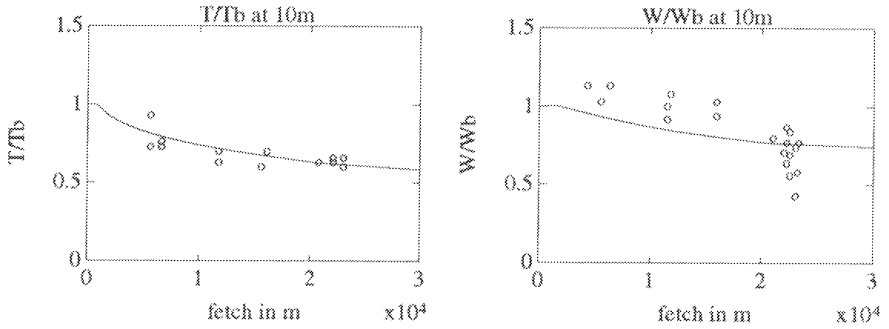

Figure 8: Distribution of the air temperature ratio $(\theta_{10} - \theta_s)/(\theta^0_{10} - \theta_s)$ (left) and the wind speed ratio U_{10}/U^0_{10} over the strait. Land temperature $\theta^0_{10} = 27^oC$, water temperature $\theta_s = 11^oC$. Open circles 'o' are observations, lines are model results.

a function of fetch across the strait is shown. Data are compiled from Gryning and Joffre (1987), their figures 1 and 2 for the unstable conditions. These conditions occurred in the day time period when the air flow from a warm landmass runs onto cold water. The observed temperature ratio decreases over the water. The wind speed ratio also decreases with fetch. On the initial stage the observed acceleration of the wind speed (the ratio exceeds 1) is not reproduced by the model. However the difference in observations and model results is rather small and is comparable to the scatter in measurements. The temperature ratio is well reproduced by the model.

3.3.3 Influence of the IBL baroclinicity on the surface wind

As was mentioned before, the pressure gradient in the IBL related to the temperature difference between land and sea surface can strongly influence the near surface wind. The known phenomenon of the near surface wind jet in the coastal zone, when the wind speed increases up to 10m/s, results from the baroclinicity effect in the IBL evolution. Such jets were observed e.g., in experiments Zemba and Friehe (1987), and Jury (1993).

The Agulhas Current experiment. Results were obtained over the ocean temperature front (Jury, 1993). However, they are of interest in the study of the coastal zone too; the roughness change across the coastal line could only increase the reported effects. In figure

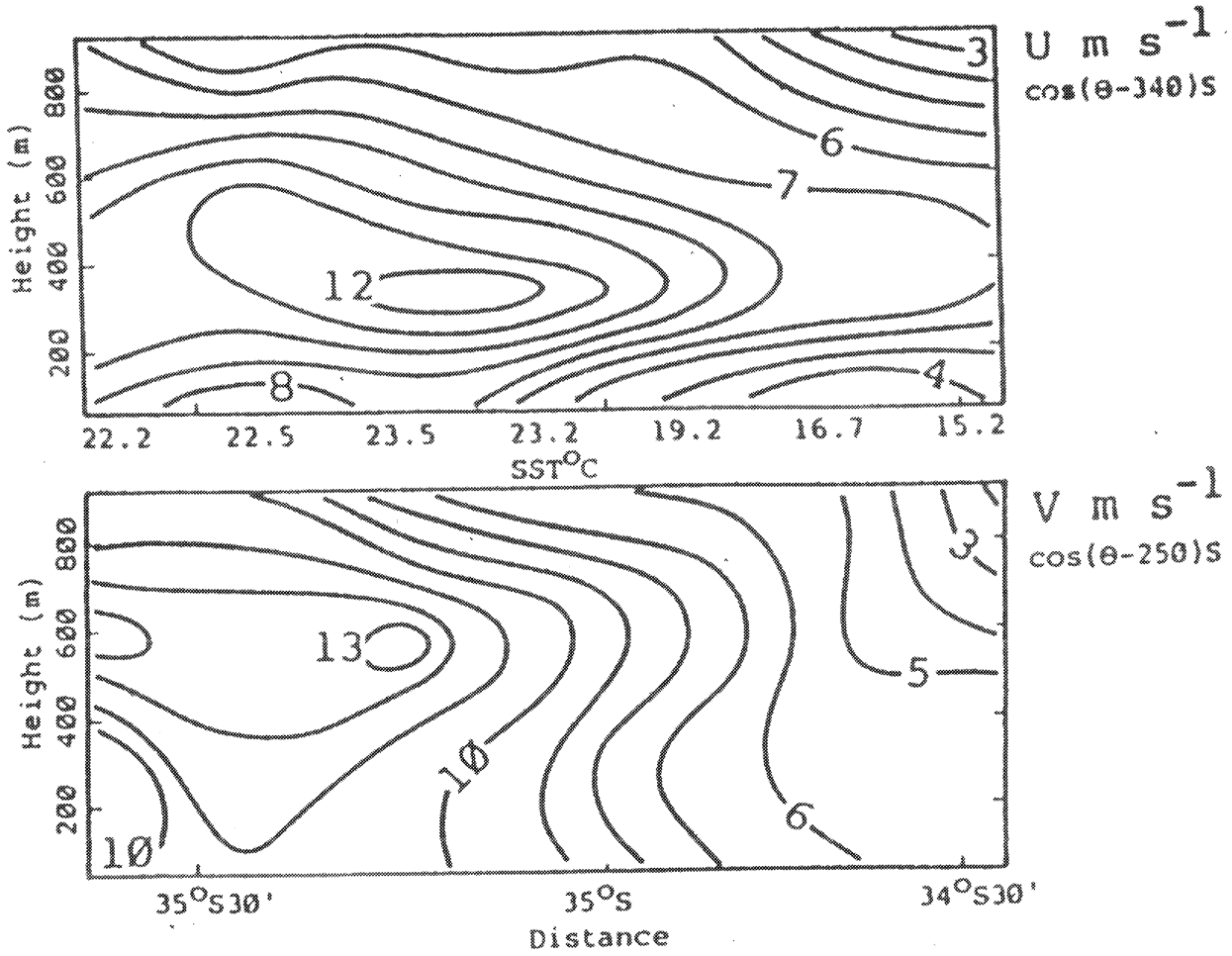

Figure 9: Cross-section structure of (top) cross-front wind component and (bottom) along-front wind component. SSTs are listed for reference. Contour interval is 1 m/s. With south to the left, the cross-front component is to the left and the along-cross component is out of the page. Compiled from Jury (1993).

9, taken from Jury (1993), the cross-section structure of cross-front and along-front wind components are presented. Observations were obtained in an aircraft experiment over the Agulhas Current temperature front, where the temperature difference across the front was up to 7°. Model calculations for the same conditions are shown in figure 10. The sea temperature difference over the front is 7°, the geostrophic wind speed is 8 m/s, the upstream air flow stratification is neutral. The model qualitatively reproduces the observations. The wind jet is generated just behind the front line and is located at the same height as the observed one. The increase of the wind speed in the jet is comparable with the observed one.

This section illustrates the fact that the baroclinicity effect in the IBL can strongly influence the near surface wind field. We have shown that our simplified model of the IBL evolution is able to reproduce such a complicated phenomenon as a wind jet resulting from a large temperature gradient across a surface discontinuity.

4 Model application

The developed model of the IBL growth will be applied here for interpretation of a radar image of a coastal zone of the Black Sea, section 4.1. In section 4.2 we shall discuss a

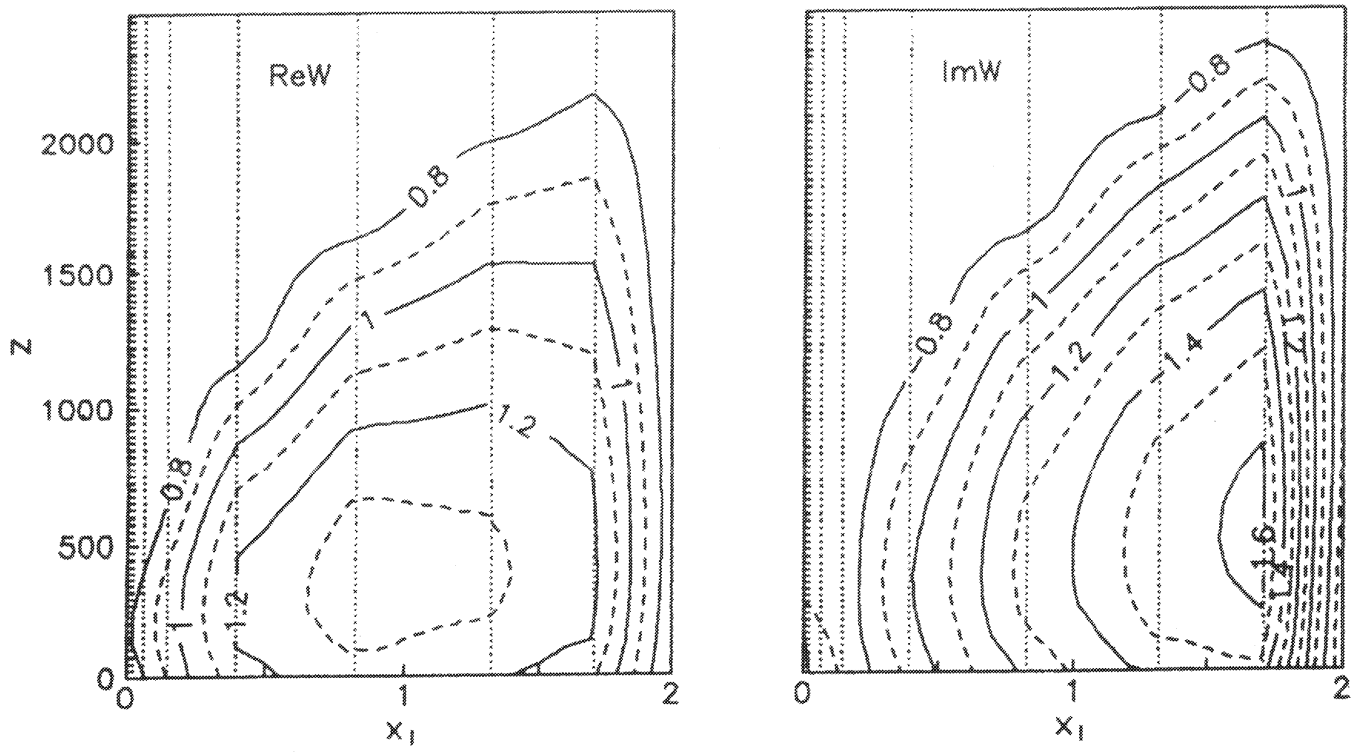

Figure 10: Cross-section structure of (left) cross-front wind component and (right) along-front wind component. The front line is at $x = 0$. Contour lines are for the wind velocity normalized on the geostrophic wind.

problem of dynamical coupling of wind waves with the atmosphere. A model of the SBL in presence of waves is introduced in section 4.2.1. Impact of wind transformation on the sea roughness parameter and wave growth is discussed in section 4.2.2. In section 4.3 we present calculations of wind transformation and wave growth for atmospheric and ocean conditions typical for the Dutch coastal zone of the North Sea.

4.1 Interpretation of a radar image

Radar observation of the sea surface is considered to be a powerful tool to study the marine boundary layer phenomena in the coastal zone. In figure 11 a radar image of the western part of the Black Sea is shown. The image is obtained from radar measurements from the Ukrainian satellite "SICH-1" (X-band, VV-polarization) on January 13th, 1995. For a X-band radar the backscatter signal is proportional to the surface wind stress. Therefore, the bright area in the image (figure 11) can be interpreted as an area of large wind stresses, and the dark area (weak backscattering) is related to small wind stresses. Thus, the 2-D spatial variations in a radar signal describe the variability of the near surface wind. One can notice a strong variability of the wind stress along the Ukrainian coast of the Black Sea (upper left corner of the image). In that period of the year a north-easterly wind was blowing from cold land into warmer sea. We shall analyze the wind field distribution along sections A and B, shown in figure 11, which is quite different. Along the A-section a strong increase of the surface stress is observed near the shore. Further on, the stress rapidly decreases with a distance from the shore. The upwind land here is very flat (Ukrainian steppe) and thus relatively smooth ($z_0 \sim 0.05$m). Along section B the distribution of the surface stress is quite opposite: the stress first drops and then increases with a distance from the shore. The upwind land here is the Crimea mountains characterized by a large roughness ($z_0 \sim 1$m).

In figures 12 and 13 the model calculations of the surface stress along sections A and B are shown. Meteorological conditions were specified according to observations. In case A stably stratified air flow (the vertical temperature gradient is $10^{-2} K^o/m$) runs from cold and flat land ($\theta_l = 0^oC$, $z_0 = 0.05$ m) onto relatively warm sea ($\theta_s = 5^oC$). Near the shore (at distances from the coast line up to 50km) the stress rapidly increases. This is due to unstable stratification over the sea at the initial stage of IBL evolution. Running further over the warm sea, the air flow is warmed up and the IBL stratification changes from unstable to neutral. As the geostrophic wind is constant, this results in a decrease of the wind stresses.

In case B stably stratified air flow (the vertical gradient is 0.5 $10^{-2} K^o/m$) runs from a very rough $z_0 = 1m$, and warm $\theta_l = 5^oC$ land onto the sea $\theta_s = 5^oC$. Due to a very rough land the surface wind is weak and the stress over the water near the shore is small as well. The surface stress increases as the IBL height attains the level where the wind speed is no more affected by the land roughness. In both cases, at a fetch of about 300 km the transfer coefficient $C_g = u_*^2/G^2$ attains its equilibrium value of $\sim 0.6\ 10^{-3}$, which is defined by the sea roughness and the geostrophic wind speed.

In this section we have shown that the model is capable to explain (at least) qualitatively the characteristic distribution of surface stress in the coastal zone as obtained from a radar image. This is a promising result as it shows the possibility of radar image interpretation

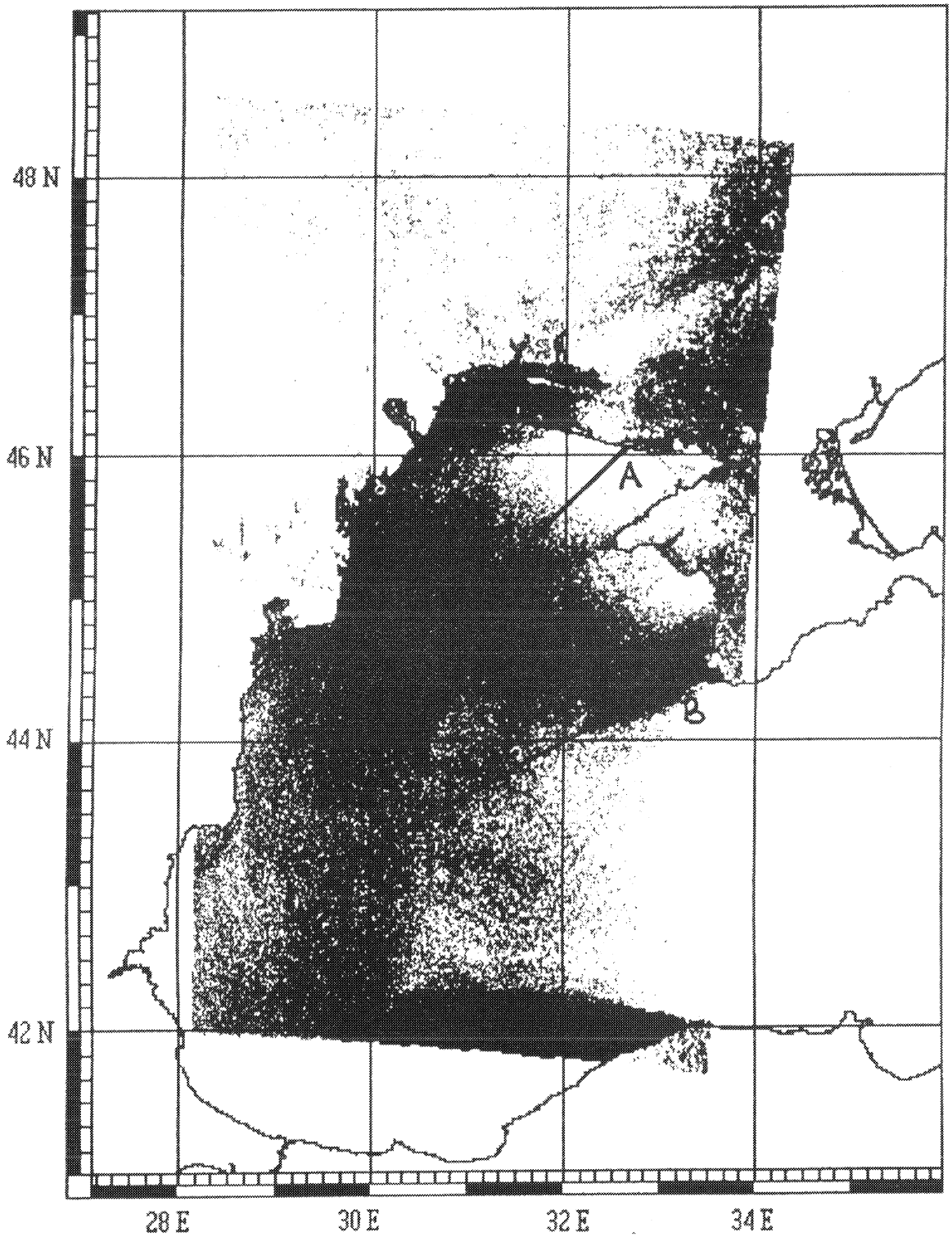

Figure 11: Radar (X-band, VV-polarization) image of the Black Sea obtained by the Ukrainian SICH-1 satellite on January 13th, 1996. Time: 13:26 GMT. Line A and B indicate sections along which the model simulation of the IBL growth is performed.

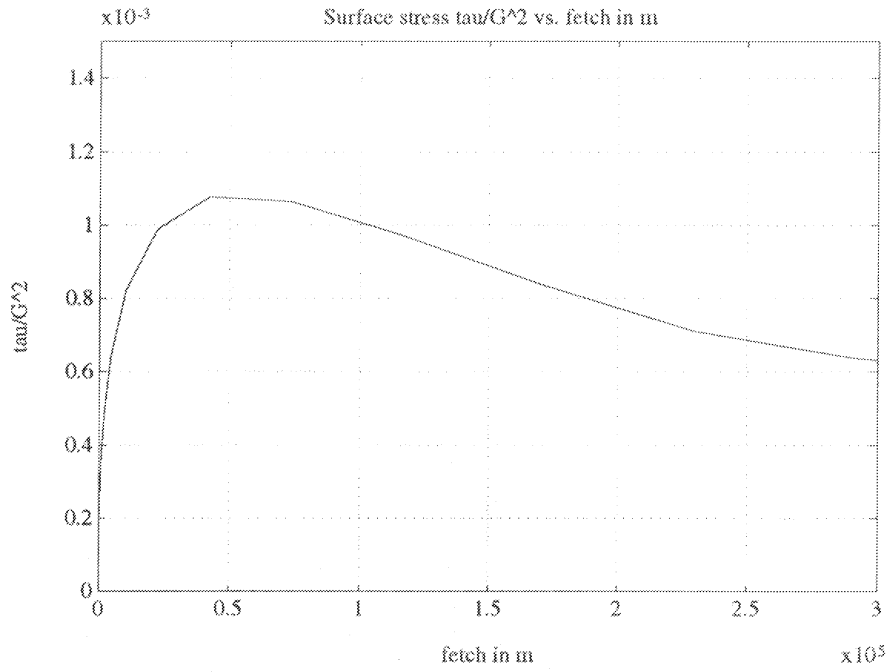

Figure 12: Calculated surface stress u_*^2/G^2 as a function of fetch. Section A (see figure 11).

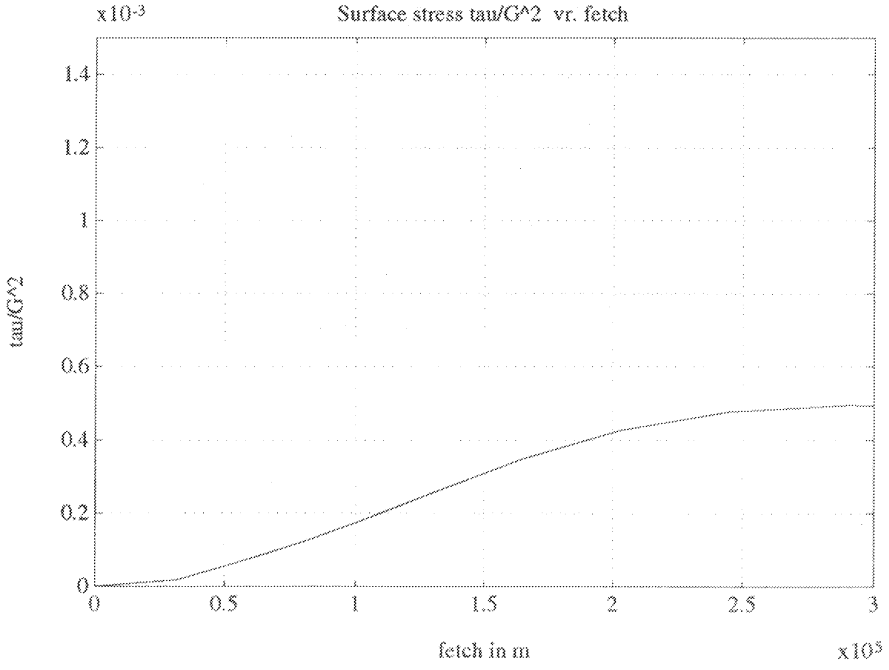

Figure 13: Calculated surface stress u_*^2/G^2 as a function of fetch. Section B (see figure 11).

with further application to the sea surface monitoring.

4.2 Dynamical coupling of waves with the atmosphere

The surface transfer processes of momentum, sensible heat and moisture are strongly affected by the movement and distortion of the ocean surface by the wind -wind waves-, because these wave motions enhance transfer rates even when the surface is fairly smooth and continuous, and further enhance them when it breaks. The bulk parameterization of the surface boundary layer relates the fluxes to the local wind speed (and atmospheric stability parameters). If the functional relation of the sea surface roughness z_0 on the wind speed (friction velocity) is known, the surface boundary layer problem can be explicitly solved to obtain the fluxes. Throughout this paper we have used the famous Charnock relation (Charnock,1955)

$$z_0 = 0.015\frac{u_*^2}{g} \tag{158}$$

for the description of the sea surface roughness. To account for light winds, relation (158) is extended to

$$z_0 = 0.015\frac{u_*^2}{g} + 0.1\frac{\nu}{u_*}, \tag{159}$$

where ν is the kinematic viscosity of the air.

Since waves grow, evolve and decay on their own dynamical time/length scales, the fluxes in general cannot be described by the local wind speed alone. In coastal regions, across atmospheric synoptic frontal zones, and in mixed wind wave-swell seas, the sea state varies rapidly in space and time. Here one may expect the momentum flux to depend both on the wind speed and the sea state. Therefore a theory that takes into account the sea state to calculate the momentum flux is required.

4.2.1 Model of the neutral SBL in presence of waves

Such a theory was introduced by Janssen (1989) and later by Chalikov and Makin (1991). The state of the sea which can be characterized by the wave spectrum $S(k,\theta)$ is explicitly taken into account in this theory to describe the exchange of momentum at the sea surface.

The approach is based on the conservation of momentum in the marine atmospheric surface boundary layer, which implies that the total stress is independent of height, so that the momentum flux at a given height is equal to the momentum flux at the sea surface. By definition this total momentum flux equals the square of the friction velocity u_*:

$$\frac{\tau}{\rho_a} = \text{Const.} = u_*^2 \tag{160}$$

The total stress τ is supported by both turbulent motions of the air τ^t and by the organised wave-induced motions due to the presence of waves τ^w:

$$\tau = \tau^t(z) + \tau^w(z) \tag{161}$$

The turbulent flux is parameterized in terms of mixing-length theory:

$$\frac{\tau^t}{\rho_a} = (\kappa z)^2 \frac{du}{dz}\left|\frac{du}{dz}\right| \tag{162}$$

The momentum flux from the atmosphere to waves can be estimated according to

$$\frac{\tau_0^w}{\rho_a} = \int_0^\infty \int_{-\pi}^{\pi} \omega^2 S\beta \cos\theta k dk d\theta, \tag{163}$$

where the wave number k satisfies the dispersion relation $\omega^2 = gk + Tk^3$ and ω is the wave frequency. The energy flux from the atmosphere to waves S_{in} is assumed to be known. It is defined in terms of the growth rate parameter $\beta(k,\theta)$, so that $S_{in} = \omega\beta S$.

The wave-induced flux τ^w decays rapidly with height. Chalikov and Makin (1991), and Chalikov and Belevich (1993) used detailed calculations of the turbulent boundary layer above waves of finite amplitude (Makin, 1989) to parameterize the vertical distribution of the wave-induced flux $\tau^w(z)$. The distribution was found to closely follow exponential decay. The exponential decay can be approximated by a step function (Chalikov and Makin, 1991; Makin et al., 1995)

$$\tau^w(z) = \tau_0^w \mathrm{He}(h_w - z), \tag{164}$$

(He(z) is a Heaviside function, He=1 at $z \geq 0$ and He= 0 at $z \leq 0$) , where the height h_w is defined by

$$h_w^{-1} = \frac{1}{\tau_0^w} \int_0^\infty \int_{-\pi}^{\pi} 2k\omega^2 S\beta \cos\theta k dk d\theta. \tag{165}$$

The resistance law of the SBL in presence of waves can be obtained from (160)-(165)

$$r_1 u_* + r_2 (u_*^2 - \tau_0^w)^{\frac{1}{2}} = U_r, \tag{166}$$

where functions r_1 and r_2 are

$$r_1 = \frac{1}{\kappa} \ln \frac{h}{h_w}, \quad r_2 = \frac{1}{\kappa} \ln \frac{h_w}{z_0^l}, \tag{167}$$

and U_r is the wind speed at the IBL height δ, if $\delta < h$, and at the height of the SBL if $h < \delta$. The wind speed U_r follows from the solution of the PBL problem. From (166) the drag coefficient of the sea surface $C_D = u_*^2/U_h^2$ is

$$C_D^{\frac{1}{2}} = \frac{1}{r_1^2 - r_2^2} \left(r_1 - r_2 [1 - \frac{\tau_0^w}{U_h^2}(r_1^2 - r_2^2)]^{1/2} \right). \tag{168}$$

The relation for the sea surface roughness then follows from (47) (assuming neutral SBL) and (166):

$$z_0 = z_0^l \left(\frac{h_w}{z_0^l} \right)^{1-\sqrt{1-\alpha_c}}, \tag{169}$$

where

$$\alpha_c = \frac{\tau_0^w}{\tau} \tag{170}$$

is the coupling parameter. The local roughness length z_0^l , which specifies the local properties of the water surface (Makin et al., 1995), is

$$z_0^l = 0.1 \frac{\nu}{u_* \sqrt{1 - \alpha_c}}. \tag{171}$$

Equation (169) relates the sea surface roughness to the state of the sea.

When equation (169) is used in the PBL model instead of the Charnock relation (159) additional knowledge of the sea wave spectra is required.

4.2.2 Role of the surface wind transformation on the wave growth

In principle, the distribution of wave spectra in the coastal zone can be obtained using a third generation coastal wave model. Such model solves the wave transport equation for the wave spectrum. They describe generation of waves by the wind, dissipation due to wave breaking and interaction with the bottom, and nonlinear interactions. However, the use of such models to study the dynamical coupling of waves with the atmosphere is beyond the scope of the present project.

We shall use here an empirical model of wave spectra to assess the consequences of dynamical coupling for the calculation of sea roughness in the coastal zone. We follow Makin et al. (1995) and use the Donelan et al. (1985), Donelan and Pierson (1987) (DP) model of a wave spectrum. In that model the wave spectrum consists of two parts. The energy containing part is proportional to the inverse wave age parameter u_{10}/c_p to the power of 0.55 (u_{10} is the wind speed at 10 metre height, c_p is the wave phase speed at the peak of the spectrum). The high frequency part which is patched to the energy- containing part at a wave number roughly 10 times the peak wave number of the fully developed spectrum, has no wave age dependence. (A detailed description of the wave spectrum model can be found in Makin et al., 1995).

In figure 14 the distribution of the roughness length z_0 as a function of fetch is shown. The roughness length is calculated according to (159) and using the coupling approach. Only the small scale evolution of the IBL is regarded. Results show that there is no difference in the distribution of the surface roughnesses. The result is not surprising and was anticipated. It was shown already in Makin et al. (1995) that the sea roughness, obtained from the wave model of Donelan et al. (1985), Donelan and Pierson (1987), turns out to be proportional to the friction velocity squared, in close agreement with the Charnock relation. It was shown also that about 90% of the wave-induced stress at the surface τ_0^w is supported by the high frequency tail of the spectrum (by waves which are shorter than 7 metres). The DP model was constructed for conditions of the open ocean. The high frequency tail of the DP model depends only on the friction velocity, and so does the roughness parameter which follows from the model.

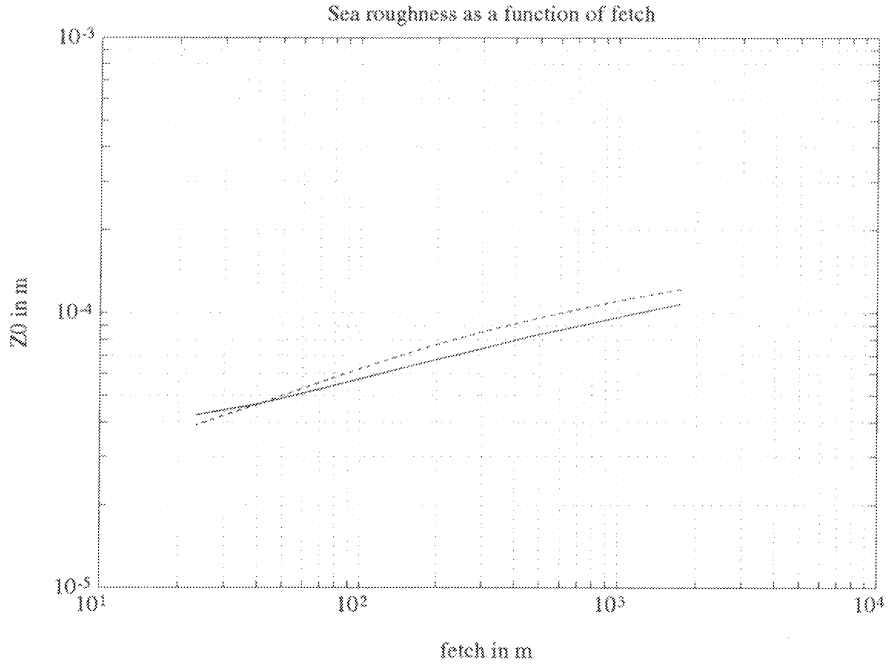

Figure 14: Sea roughness as a function of fetch. Wind speed $U_{10} = 15$ m/s. Solid line - the coupling approach, dashed - the Charnock relation (159).

In the coastal (shallow water) zone, the high frequency part of the wave spectrum is very likely to depend on more external parameters than the friction velocity alone. Unfortunately, the behaviour of the high frequency tail has not been the subject of extensive experimental verification and very little is known about its form, especially in shallow water. The existing evidence is contradictory (see discussion on the form of the high frequency tail in Makin et al. (1995)).

The study of the high frequency part of the wave spectrum is beyond the scope of this project. Instead of speculating on its form we shall use a much simpler approach to assess the impact of the wind transformation on the wave growth in the coastal zone.

For that we shall use the empirical relations for dimensionless energy $\tilde{E}$ as a function of dimensionless fetch $\tilde{X} = Xg/U_{10}^2$ obtained by Donelan et al. (1985):

$$\alpha_c \equiv \frac{U_{10}}{c_p} = 11.6\tilde{X}^{-0.23}, \tag{172}$$

$$\tilde{E} = 0.00274\alpha_c^{-3.3} \tag{173}$$

We first calculate dimensionless fetches and energies using a constant value of the wind velocity U_{10}. This is commonly done in coastal wave models when the measured velocity over land is extrapolated without any change over water. In our model the 'measured' velocity corresponds to the velocity at 10m height of the background atmosphere over land.

The significant wave height H_s

$$H_s = 4\sqrt{\tilde{E}\frac{U_{10}^4}{g^2}} \tag{174}$$

is then retrieved as a function of fetch X. Calculations are repeated using a distribution of wind velocity resulting from a solution of the IBL transformation across a coastal line. Results of both calculations are compared with each other and will be shown in the next section.

4.3 Transformation of wind and the wave growth in the coastal zone

In this section the model is applied to assess the role of the IBL evolution on the transformation of wind and the wave growth in the coastal zone. Characteristic values of the land roughness, land and sea temperatures correspond to typical conditions observed at the Dutch coastal zone of the North Sea. Presented are the wind speed and air temperature at 10m height, angle of the wind direction over the sea relative to the wind direction over land, and the significant wave height calculated according to formulas (172)-(174). Rather strong wind is considered as extreme conditions are of great interest for practical applications.

4.3.1 Case 1: Wind transformation in neutral conditions

Neutral conditions are typical for the late spring and early autumn when the sea, the land and the air have approximately the same temperature. Model calculations are presented in figure 15. The land temperature θ_l, the sea temperature θ_s, and the air temperature θ_a (θ_a relates to the temperature of the free atmosphere at $z = 1000$m height) all are taken to be 15^oC, the geostrophic wind speed is $G = 25$m/s and the surface roughness is assumed to be $z_{0l} = 0.1$m. This roughness corresponds to farmland with long grass, few trees, and many hedges. The wind speed over land is 9 m/s. The wind accelerates over the sea due to the relatively smooth sea surface, without changes in its direction. At a fetch of 100km the wind speed increases to 12 m/s, which is 30% of the wind speed over land. The significant wave height H_s calculated with a constant wind speed is up to 0.5m (or 50%) lower than the one calculated with the wind changing with distance from the shore.

4.3.2 Case 2: Wind transformation over warm sea

This condition is typical for late autumn or early winter when the sea is significantly warmer than the land and the atmosphere. Model calculations presented in figure 16 are for $\theta_l = \theta_a = 5^oC$, $\theta_s = 15^oC$. The wind speed and the surface roughness remain the same as in section 4.3.1. In this case the wind speed increases significantly (from 9 to 17 m/s) over the sea due to the acceleration of the air flow. The acceleration occurs due to the combined action of the smooth sea surface and unstable stratification over the sea. Unstable conditions over the sea lead to strong vertical convective mixing that increases the wind speed in the

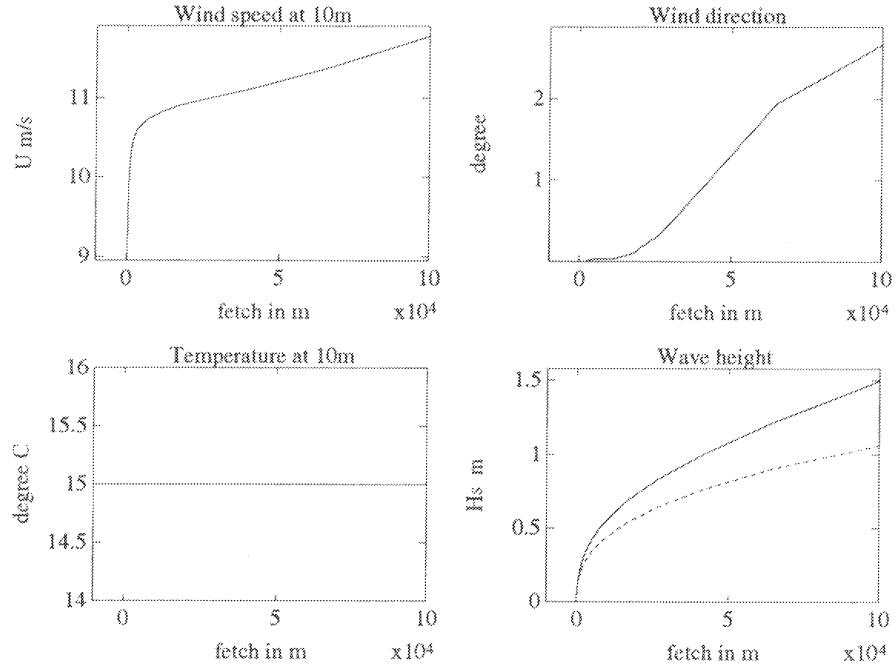

Figure 15: Transformation of wind and wave growth for neutral conditions. $G = 25$m/s, $\theta_l = 15^oC$, $\theta_s = 15^oC$, $\theta_a = 15^oC$, $z_{0l} = 0.1$m.

lower part of the boundary layer. The IBL transformation occurs with a noticeable rotation of the wind and warming of the air. After 25 km from the shore the wind speed is already twice as large as over land. This is a significant increase which results in a significant wave height twice larger than that with a constant wind speed of 9 m/s. Such an increase in H_s is significant for coastal applications.

4.3.3 Case 3: Wind transformation over cold sea

This condition is typical for daytime in the summer, when the sea is colder than the land and the atmosphere. Model calculations presented in figure 17 are performed with $\theta_l = \theta_a = 25^oC$, $\theta_s = 15^oC$. In this case, the wind speed decreases over the sea due to stable atmosphere conditions over the sea. Though the air flow tends to accelerate over the smooth sea surface, the stratification effect dominates and the wind speed reduces with fetch. The wind speed decreases from 9 to 7 m/s and the wind turns to the left relative to the coastal line. The air cooling is significant. The temperature drops up to 10^o at large distances from the shore. In this case the significant wave height calculated with a constant wind is higher. Notice that the effect of the IBL transformation is not so pronounced in this particular case due to the fact that the acceleration of wind speed over the smooth sea surface is compensated by the deceleration of wind speed caused by the influence of stratification.

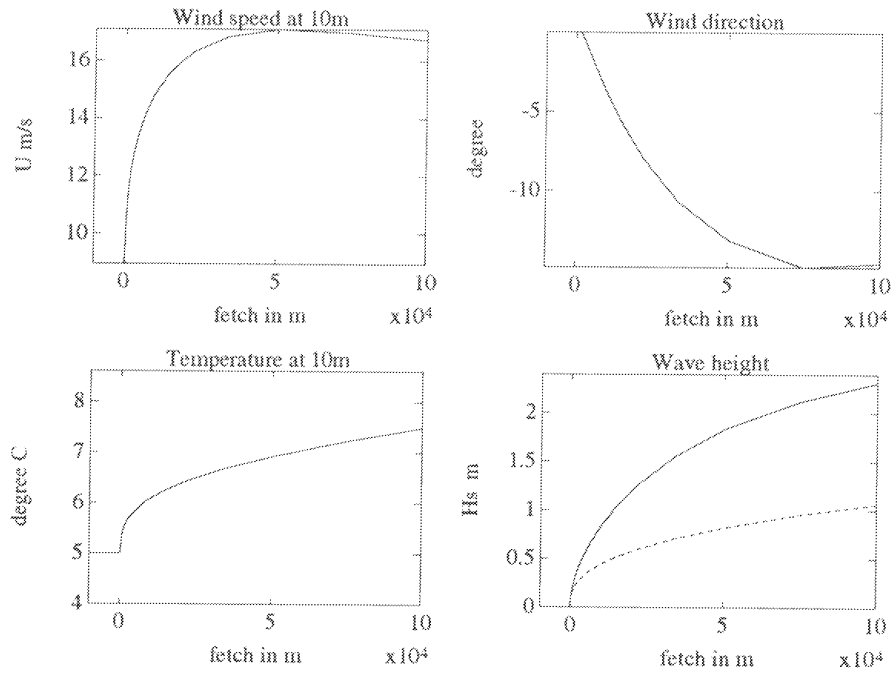

Figure 16: Transformation of wind and wave growth over a warm sea. $G = 25\mathrm{m/s}$, $\theta_l = 5°C$, $\theta_s = 15°C$, $\theta_a = 5°C$, $z_{0l} = 0.1\mathrm{m}$.

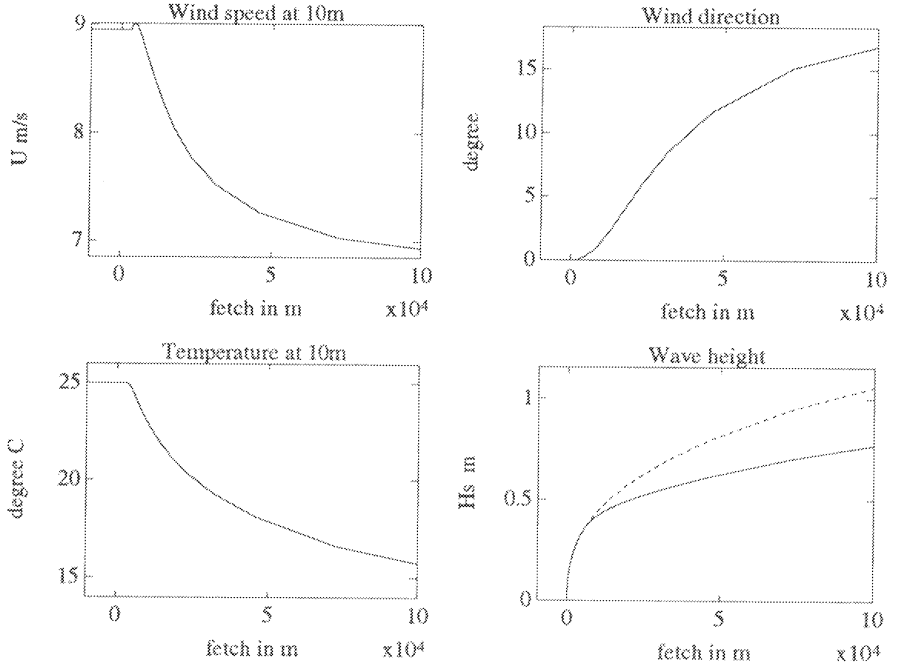

Figure 17: Transformation of wind and wave growth over a cold sea. $G = 25\mathrm{m/s}$, $\theta_l = 25°C$, $\theta_s = 15°C$, $\theta_a = 25°C$, $z_{0l} = 0.1\mathrm{m}$.

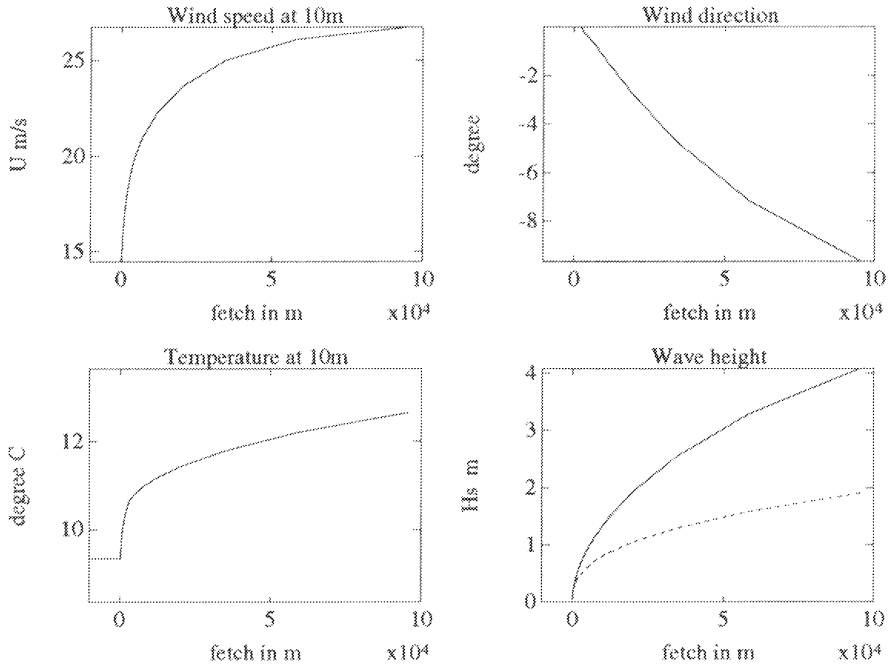

Figure 18: Transformation of wind and wave growth over a warm sea and a stably stratified atmosphere. $G = 50\text{m/s}$, $\theta_l = 5^oC$, $\theta_s = 15^oC$, $\theta_a = 15^oC$, $z_{0l} = 0.1\text{m}$.

4.3.4 Case 4: Wind transformation over warm sea and stably stratified atmosphere

During the day cycle in the summer the daytime conditions (case 3) could significantly change in the night. Due to infrared emission, the land surface during nighttime cools and becomes colder than the sea. This process is usually accompanied by the formation of stable stratification in the atmosphere. Similar conditions could also be realized when a synoptic warm front crosses cold land and warm sea. Typical temperatures could be: $\theta_l = 5^oC$, $\theta_a = 15^oC$, $\theta_s = 15^oC$. Model results are presented in figure 18 for a geostrophic wind speed $G = 50\text{m/s}$. The surface roughness remains $z_{0l} = 0.1\text{m}$. As soon as the air flow moves onto the sea, a convective IBL begins to develop. Similar to case 2, the wind speed significantly increases over sea. This is due to the acceleration of the lower part of the boundary layer caused by the smooth sea surface and unstable stratification connected with the intensive vertical convective mixing in the IBL. The wind speed increases approximately to twice its value over land. In this case the significant wave heights H_s, calculated with a constant wind of 15 m/s over land, is up to 2 times lower than that calculated with a changing wind speed. During the day cycle, changes in land temperature could significantly modify profiles of wind speed and temperature, and could have a pronounced impact on wave growth in the coastal zone.

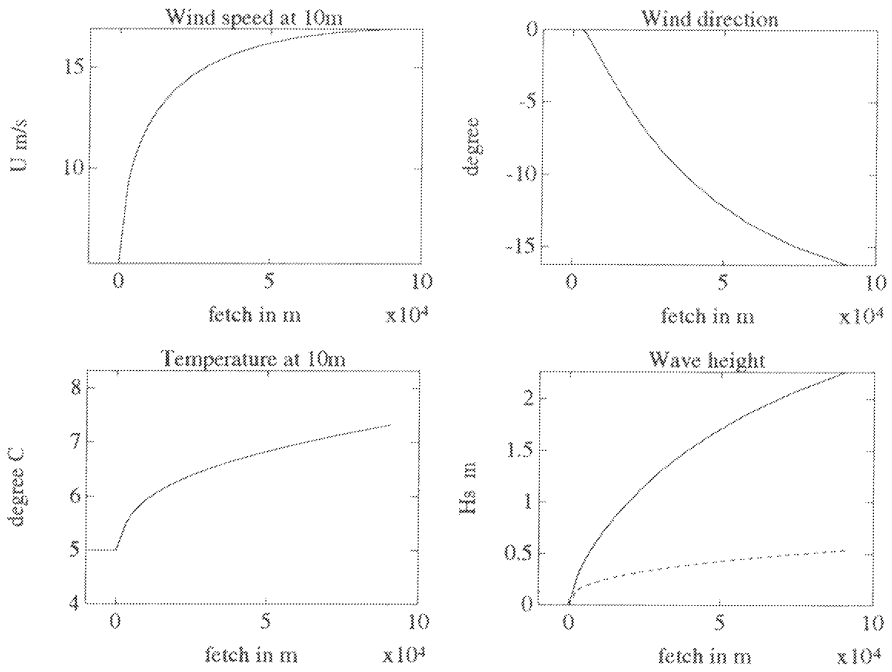

Figure 19: Transformation of wind and wave growth over a warm sea. $G = 25\text{m/s}$, $\theta_l = 5^oC$, $\theta_s = 15^oC$, $\theta_a = 5^oC$, $z_{0l} = 1\text{m}$.

4.3.5 Case 5: Influence of the land roughness

To estimate the influence of the land roughness on the wind transformation and wave growth, the model calculation are performed with $z_{0l} = 0.01\text{m}$ and $z_{0l} = 1\text{m}$ for air flow over warm sea (see case 2). For this case, the effect of the IBL transformation on wind and temperature profiles, and on wave growth, is very pronounced.

In figure 19 and 20 the results are shown for land roughness $z_{0l} = 1\text{m}$ and $z_{0l} = 0.01\text{m}$, respectively. Temperatures and wind speed correspond to case 2: $\theta_l = 5^oC$, $\theta_a = 5^oC$, $\theta_s = 15^o$, $G = 25\text{m/s}$. Comparing the results presented in figures 16, 19 and 20, we find that the parameters of the boundary layer are very close to each other starting from fetch of about 25km. It shows that the structure of the IBL is formed mainly by the local sea surface and does not depend significantly on the land roughness. The difference between parameters obtained for the various land roughness occurs only at small fetches, where the IBL 'feels the land' through the wind profile in the lower part of the background boundary layer.

However the distribution of significant wave height is quite different for all three cases. The prediction of wave heights based on land wind significantly depends on land roughness. The reason for that is trivial, however. The larger land roughness correspond to lower wind speeds over land. That results in a large difference in significant wave height calculated with a constant wind speed over land and with a changing wind due to the IBL evolution. For the land roughness $z_{0l} = 1m$ this difference is drastic, significant wave height calculated with

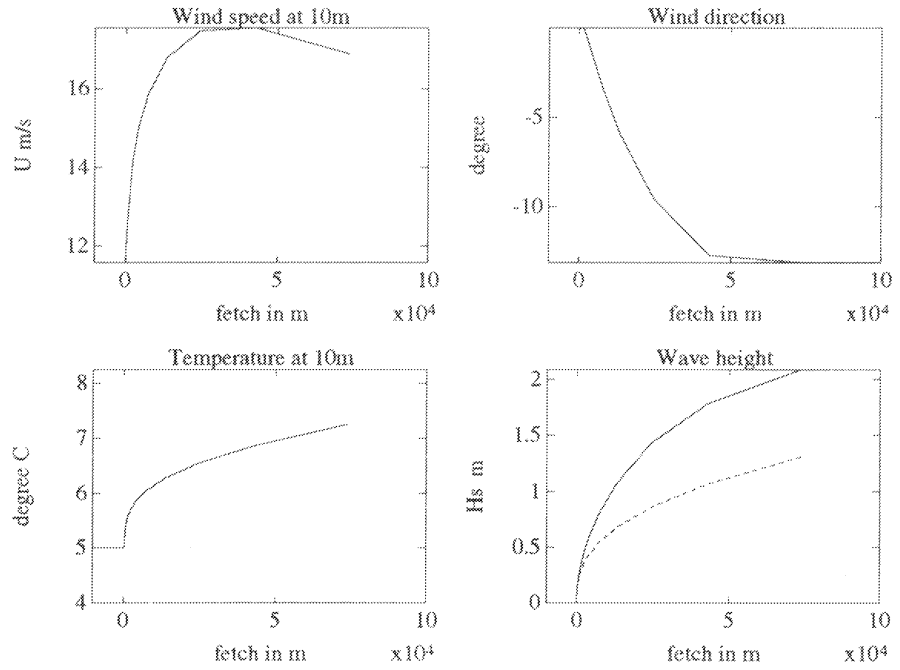

Figure 20: Transformation of wind and wave growth over a warm sea. $G = 25\text{m/s}$, $\theta_l = 5^oC$, $\theta_s = 15^oC$, $\theta_a = 5^oC$, $z_{0l} = 0.01\text{m}$.

a constant wind speed is to 5 times lower.

In this section we have shown that the wind and temperature fields change drastically in the coastal zone. For many engineering applications in the coastal zone this changes have to be accounted for.

5 Conclusions

We have presented a simplified physical model of the PBL describing effects which abrupt changes in surface roughness and temperature in the coastal zone have on wind velocity. The model is based on the concept of the IBL growth and similarity approach. A 3-layer eddy-viscosity model is used for the description of the PBL structure in presence of a developing IBL. Similarity approach is used to describe the structure of the IBL developing inside the SBL and in the Ekman part of the PBL. A generalized equation for the IBL height growth is suggested which allows for a consistent description of the small scale and mesoscale evolution of the IBL.

The model describes the transformation of wind across a coastal line (off-shore and on-shore winds) and across land- sea-land or sea-land-sea domains.

The model is verified on existing observations. The model results are in a reasonable agreement with experiments.

The simulation of the Øresund experiment reveals the importance of stratification effects

on the wind transformation over sea. The possibility of describing the jet wind due to the baroclinicity effect in a developing IBL is shown by simulating the Agulhas Current experiment.

The interpretation of a radar image of the coastal zone of the Black Sea gives an example of model application in the remote monitoring of the sea surface.

Dynamical coupling of wind waves with the atmosphere is an option of the model. The impact of the wind transformation on wave growth is discussed.

The model is used to assess the impact of the IBL evolution on the transformation of wind and wave growth in the coastal zone for conditions typical for the Dutch coast of the North Sea. The wind speed over sea could increase to as much as twice its value over land. A difference of up to five times in significant wave height, obtained with a constant wind speed over land and with wind changing along the fetch, is reported.

Model results show that the wind field changes drastically in the coastal zone. Most of the models of water dynamics are driven by surface wind (stress). For many applications it is necessary to account for the wind transformation in the coastal zone. The (relative) simplicity of this model makes it attractive for engineering applications in modelling hydrophysical processes and atmospheric flows in the coastal zone.

6 Acknowledgements

The first author is grateful for the financial support he received from the Netherlands Organisation for Scientific research (NWO) to carry out the project. The research was performed at the Royal Netherlands Meteorological Institute (KNMI). Our special acknowledgements are for Jeanette Onvlee for her strong support of the project and attention to our work.

References

[1] Bergstrom, H.A.: 1985, 'Simplified boundary layer wind model for practical applications', *J. Clim. Appl. Meteorol.*, **25**, 813-823.

[2] Bergstrom, H.A., Johansson, P.E., and A.S. Smedman: 1988, 'A study of wind speed modification and internal boundary layer heights in a coastal region', *Boundary-Layer Meteorol.*, **42**, 313-335.

[3] Brown, R. A.: 1982, 'On two-layer models and the similarity functions for the PBL', *Boundary- Layer Meteorol.*, **24**, 451-463.

[4] Bradley E.F.: 1968, 'A micrometeorological study of velocity profiles and surface drag in the region modified by a change in surface roughness', *Quart. J. Roy. Meteorol. Soc.*, **94**, 361-379.

[5] Chalikov, D.V. and Belevich, M.Yu.: 1993, 'One- dimensional theory of the wave boundary layer', *Boundary- Layer Meteorol.*, **63**, 65-96.

[6] Chalikov, D.V. and Makin, V.K.: 1991, 'Models of the wave boundary layer', *Boundary-Layer Meteorol.*, **56**, 83-99.

[7] Charnock, H.: 1955, 'Wind stress on a water surface', *Quart. J. Roy. Meteorol. Soc.*, **81**, 639- 640.

[8] Deardorff, J.W.: 1972, 'Numerical investigation of neutral and unstable planetary boundary layers', *J. Atmos. Sci.*, **29**, 91-115.

[9] Doran, J.C. and Gryning S.E.: 1987, 'Wind and temperature structure over a land-water-land area', *J. Clim. Appl. Meteorol.*, **26**, 973-979.

[10] Dyer, A.J.: 1974, 'A review of flux-profile relations', *Boundary-Layer Meteorol.*, **7**, 363-372.

[11] Elliot, W.P.: 1958, 'The growth of the atmospheric internal boundary layer', *Trans. Amer. Geophys. Un.*, **39**, 1048-1054.

[12] Garratt J.R.: 1987, 'The stable stratified internal boundary layer for steady and diurnally varying offshore flow', *Boundary- Layer Meteorol.*, **38**, 369-394.

[13] Garratt, J.R.: 1990, 'The Internal Boundary Layer - A review', *Boundary-Layer Meteorol.*, **50**, 171-203.

[14] Garratt, J.R. and B.F.Ryan: 1989, 'The structure of the stably stratified internal boundary layer in offshore flow over the sea', *Boundary-Layer Meteorol.*, **47**, 17-40.

[15] Garratt, J.R., Hess, G.D., Physick, W.L. and P. Bougeault: 1996, 'The atmospheric boundary layer - advances in knowledge and application', *Boundary-Layer Meteorol.*, **78**, 9-37.

[16] Grining, S.E.: 1985, 'The ØRESUND experiment - A nordic mesoscale dispersion experiment over a land-water-land area', *Bull. Americ. Meteorol. Soc.*, **66**, 1403-1407.

[17] Grining, S.E. and S. Joffre: 1987, 'The ØRESUND experiment,- *Proc.Workshop II, Uppsala, Sweden, Oct.13-14.*, 11-19.

[18] Janssen, P.A.E.M.: 1989, 'Wave-induced stress and the drag of air flow over sea waves', *J. Phys. Oceanogr.*, **19**, 745-754.

[19] Jensen S.E., Petersen E.L. and I. Troen: 1984, 'Extrapolation of mean wind statistics with special regard to wind energy applications', *World Meteorol.Org.*, **WCP-86**, 85 pp.

[20] Jury, M.R.: 1993, 'A thermal front within the marine atmospheric boundary layer over the Agulhas Current south of Africa: composite aircraft observation', *J. Geophys. Res.*, **C99**, 3297-3304.

[21] Kazansky, A.B. and Monin, A.S.: 1960, 'On turbulent regime above near-surface air layer', *Izv. Akad. Nauk SSSR, Ser. Geophys.*, **1**, 165-168.

[22] Kudryavtsev, V.N.: 1995, 'A model of atmosphere boundary layer transformation above sea surface temperature front', *Morskoy Hydrof. Zurnal*, **2**, 24-51.

[23] Landau L.D. and Lifshits E.M.: 1959, *Fluid Mechanics*, Addison-Wesley, Reading, Mas., 536 pp.

[24] Makin, V.K.: 1989, 'The dynamics and structure of the boundary layer above sea', *Senior doctorate thesis*, Inst. Oceanology, Acad. Sci. USSR, Moscow, 417 pp.

[25] Makin, V.K., Kudryavtsev, V.N. and C. Mastenbroek: 1995, 'Drag of the sea surface', *Boundary-Layer Meteorol.*, **73**, 159-182.

[26] Mason, P.J.: 1994, 'Large-eddy simulation: a critical review of the technique', *Quart. J. R. Meteorol. Sci.*, **120**, 1-26.

[27] Meroney, R.W., Cermak, J. E. and Yang, B.T.: 1975, 'Modeling of atmospheric transport and fumigation at shoreline sites', *Boundary-Layer Meteorol.*, **9**, p.69-90.

[28] Monin, A.S. and Obukhov, A.M.: 1954, 'Main laws of turbulent mixing in near-surface layer of atmosphere', *Trudy Geophys. Inst. Akad. Nauk*, **24(151)**, 163-187.

[29] Mulhearn P.J.: 1977, 'Relations between surface fluxes and mean profiles of velocity, temperature and concentration, downwind of a change in surface roughness' *Quart. J. Roy. Meteorol. Soc.*, **103**, 785-802.

[30] Mulhearn, P.J.: 1981, 'On the formation of a stably stratified internal boundary layer by advection of warm air over a cooler sea', *Boundary-Layer Meteorol.*, **21**, 247-254.

[31] Panofsky, H. and J. Dutton: 1984, *Atmospheric Turbulence*, Academic, San Diego, Calif., 397 pp.

[32] Raynor G.S., P. Michael, R.M.Brown, and S. Sethuraman: 1975, 'Studies of atmospheric diffusion from a nearshore oceanic site', *J. Appl. Meteorol.*, **7**, 331-348.

[33] Raynor, G.S., Sethuraman, S. and Brown, R.M.: 1979, 'Formation and characteristics of coastal internal boundary layers during onshore flows' *Boundary-Layer Meteorol.*, **16**, 487-514.

[34] Rossby C.G. and Montgomery R.: 1935, 'The layers of frictional influence in wind ocean currents', *MIT paper* **3**, 3-101.

[35] Schlichting, H.: 1979, *Boundary Layer Theory*, McGrow-Hill, New York and London, 817 pp.

[36] Tennekes H.: 1973, 'A model for the dynamics of the inversion above a convective boundary layer', *J. Atmos. Sci.*, **30**, 558-567.

[37] Townsend A.A.: 1965, 'The response of a turbulent boundary layer to abrupt changes in surface conditions', *J. Fluid Mech.*, **22**, 799-822.

[38] Taylor P.A.: 1971, 'Airflow above changes in surface heat flux, temperature and roughness: An extension to include the stable case', *Boundary-Layer Meteor.*, **1**, 474-497.

[39] Taylor P.A. and R.J. Lee: 1984, 'Simple guidelines for estimating wind speed variations due to small scale topographic feature', *Climatol. Bull. Canadian Meteorol. Oceanogr. Soc.*, **18**, 3-32.

[40] Van Wijk A.J.M., A.C.M. Beljaars, A.A.M. Holtslag and W.C. Turkenburg: 1990, 'Diabatic wind speed profiles in coastal regions: comparison of an internal boundary layer (IBL) model with observations', *Boundary- Layer Meteorol.*, **51**, 49-75.

[41] Venkatram A.A.: 1977, 'Model of internal boundary-layer development', *Boundary-Layer Meteorol.*, **11**, 419-438.

[42] Walmsley J.L.: 1989, 'Internal boundary layer height formulate - A comparison with atmospheric data', *Boundary-Layer Meteorol.*, **47**, 251-262.

[43] Zemba J. and C.A. Friehe: 1987, 'The marine atmospheric boundary layer jet in the coastal ocean dynamic experiment', *J. Geophys. Res.*, **92**, 1489-1496.

[44] Zilitinkevich, S.S.: 1970, *Dynamics of the Atmospheric Boundary Layer*, Gidrometeoizdat, Leningrad, 292 pp.

[45] Zilitinkevich, S.S.: 1989a, 'Velocity profiles, resistance law and the dissipation rate of mean flow kinetic energy in a neutrally and stably stratified Planetary Boundary Layer', *Boundary-Layer Meteorol.*, **46**, p.367-387.

[46] Zilitinkevich, S.S.: 1989b, 'The temperature profile and heat transfer law in neutrally and stably stratified Planetary Boundary Layer', *Boundary-Layer Meteor.*, **49**, 1-6.

[47] Yaglom, A.M.: 1977, 'Comments on wind and temperature flux-profile relationships', *Boundary-Layer Meteor.*, **11**, 89-102.